Build Simul (2025) 18: 99–121
https://doi.org/10.1007/s12273-024-1195-5

The mutual impacts of individual building design and local microclimate in high-density cities and the major influential parameters

Zeming Zhao[1], Hangxin Li[1,2] (✉), Shengwei Wang[1,3] (✉)

1. Department of Building Environment and Energy Engineering, The Hong Kong Polytechnic University, Hong Kong, China
2. Shenzhen Research Institute, The Hong Kong Polytechnic University, Shenzhen, China
3. Research Institute for Smart Energy, The Hong Kong Polytechnic University, Hong Kong, China

Abstract

Development of individual building in existing district is common in high-density cities due to the limited space. Such development affects the local microclimate naturally, but the interaction is ignored in current building design practices. In this study, a comprehensive and systematic analysis is conducted to investigate the mutual impacts between new individual building design and local microclimate considering the interaction, and to identify the major influential building parameters on both local microclimate and building energy performance in subtropical urban area. A large number of high-resolution microclimate and building simulations are performed based on advanced GIS spatial analysis techniques under different building designs for the assessment of mutual impacts. A global sensitivity analysis is conducted to identify the major influential building parameters. The results show that different building designs lead to significant variation of local wind velocity (i.e., −0.95 to +4.51 m/s) and air temperature (i.e., −0.60 to +1.17 K), while the local microclimate results in a change in the building energy consumption from −41.75 to 291.54 kJ/m^2. The major influential parameters on both pedestrian thermal discomfort and building energy performance are building height and overall heat transfer coefficient of the building envelope. This study provides valuable references for new building or rebuilding design in order to facilitate carbon neutrality and enhance thermal comfort in urban area.

Keywords

building-microclimate interaction
urban microclimate
building energy performance
sensitivity analysis
building design

Article History

Received: 25 June 2024
Revised: 20 September 2024
Accepted: 22 September 2024

1 Introduction

The world has been experiencing rapid urbanization in the past decades. Currently, around 56% of global population live in urban areas, and this percentage will continue to increase to 61% by 2030 according to the United Nations (Sun et al. 2020). In order to cope with the increase in population and improve the quality of the living environment, new building development or building renewal becomes common in the high-density cities. The new development could modify the ambient local microclimate, such as block the wind flow and affect the heat removal. One of the major phenomena is the urban heat island (UHI) effect. An UHI refers to an urban area with higher temperature than its rural surroundings. The UHI could contribute to thermal discomfort of urban residents and even heat-related illnesses. Therefore, much attention has been paid to the local microclimate affected by the building design.

In the past decade, increasing efforts have been made on investigating the impacts of district design on the local microclimate (Middel et al. 2014; Ali-Toudert and Böttcher 2018; Sezer et al. 2023). According to the analysis results, the design of district can have significant impacts on surrounding local microclimate at different climate conditions. For instance, the local air temperature was increased by up to 6 K in Constantine, Algeria with a Mediterranean climate (Bourbia and Boucheriba 2010). Not only the morphology but also the thermal characteristics have effect on the surrounding local microclimate. The variations of district morphology can result in the increase of local air temperature up to 2.5 °C in Zürich, Switzerland (Allegrini and Carmeliet

E-mail: hangxin.li@polyu.edu.hk (Hangxin Li); beswwang@polyu.edu.hk (Shengwei Wang)

List of symbols

3D	3-dimentional	PET_n	neutral physiological equivalent temperature
C_μ	model constant	RANS	Reynolds-averaged Navier-Stokes
CFD	computational fluid dynamics	SPEA	Spearman correlation coefficient
D_{discom}	pedestrian thermal discomfort degree	TMY	typical meteorological year
DO	discrete ordinates	UHI	urban heat island
GIS	geographic information systems	U_s	velocity at the reference height
I_z	turbulent intensity	U_z	vertical velocity profile
k_z	turbulent kinetic energy	z	vertical coordinate
l_z	turbulence integral length	z_s	reference height
PET_{ave}	average PET	α	power-law exponent
PET_{female}	PET of female	ε_z	turbulence dissipation
PET_{male}	PET of male		

2017). The application of cooling material with high albedo on building envelope design can lead to the decrease of local air temperature up to 0.7 °C in Thessaloniki, Greece (Tsoka 2017).

The representative studies are selected in Table 1. The methods used to quantify the impacts can be classified into two categories, i.e., on-site monitoring and simulation. The simulation software includes FLUENT, STEVE, UWG, SOLENE, OpenFOAM and ENVI-met. The studied period varies from a selected hour to one year. For instance, Li et al. (2023) evaluated microclimate performances in three typical types of residential public spaces, and investigated their relationship with surrounding microclimate during summertime heat waves. Dimoudi et al. (2013) conducted the on-site monitoring of local air temperature and wind velocity under the variations of district geometry and street configuration in urban district in Greece, Serres in a summer month. Bueno et al. (2013, 2014) utilized the UWG to predict the local air temperature in urban district with different urban parameters settings in Switzerland, France and Singapore. Though the UHI effect can be estimated by the UWG in different climates, the simplifications and assumptions of the parametric model prevent it from capturing very site-specific microclimate effects. It can be observed that existing studies mainly investigate the impacts of district design rather than individual building design on the local microclimate (Ali-Toudert and Böttcher 2018). Only limited samples are used for monitoring or simulation of local microclimate to investigate the impacts of district design. Simplified geometry model of the neighborhood/district is usually used while ignoring the real terrain (Ali-Toudert and Böttcher 2018).

At the meanwhile, the impacts of local microclimate can also impact on the building performance significantly in different climate conditions and concerning different building types (Xie et al. 2020). For instance, when the local air temperature was increased by around 1.1–1.2 K, the building cooling load was increased by 5% in Zürich, Switzerland with a temperate maritime climate (Mosteiro-Romero et al. 2020), but by up to 41% in Milan, Italy with a Mediterranean climate (Paolini et al. 2017). In Rome, the variation of the local microclimate increased the cooling load by up to 74% in residential buildings, while by 53% in office buildings (Zinzi et al. 2018).

The representative studies are summarized in Table 2. The climate condition investigated varies from temperate to tropical, and from continental to maritime. Building cooling and heating loads are the major building performance concerned. A few studies also investigated the impacts on cooling/heating degree days, indoor air temperature, dehumidification load, and night ventilation cooling potential (Paolini et al. 2017; Xie et al. 2020; Shen et al. 2021). Simulation method is usually adopted to quantify the impacts. The simulation software includes IES-VE, TRNSYS, EnergyPlus, DeST, City Energy Analyst, WUFI Plus, BuildSysPro and Citysim. The simulation period varies from a typical day to several years. For instance, Ge et al. (2023) investigated the effects of the vertical meteorological pattern on the building heating and cooling energy demands for high-rise buildings, which lead to an increase of heating load 0.7–1.6 kWh/m^2 (16%–52%) and an increase of cooling load 0.0–0.1 kWh/m^2 (0–1%) in the residential blocks in Xi'an, China. Guattari et al. (2018) utilized TRNSYS to simulate the cooling and heating energy demand of a reference building in order to investigate the effect of UHI on building energy performance in Rome, Italy. Two-year monitored weather data in suburban area and urban center were used for the estimation of UHI effect. Cui et al. (2017) investigated the impact of UHI effect on cooling and heating load of a reference building in Beijing, China using DeST. One-year

Table 1 Representative studies on the impacts of building design on local microclimate

Reference	Location and climate	Building-related factors concerned	Research scale	Quantification method	Period	Impacts on microclimate
Ge et al. 2023	Xi'an, China; Temperate continental	Land area, floor area ratio, building density, average building height, height fall, enclosure degree, sky view factor	District	On-site monitoring	6 typical sunny days	*T*: −0.8 K; WS: +0.2 to +0.8 m/s
Deng et al. 2023	Guangzhou, China; Subtropical humid	Sky view factor, building coverage ratio	District	On-site monitoring	2 days	*T*: +1.76 to +2.89 K; WS: −0.75 to −0.53 m/s
Li et al. 2023	Hong Kong, China; Subtropical humid	Three types of public spaces	District	On-site monitoring	Summer days	*T*: +0.75 to +2.14 K; RH: −5.01% to 1.85%; WS: 0 to +0.27 m/s
Ali-Toudert and Böttcher 2018	Mannheim, Germany; Temperate continental	Thermal insulation, thermal inertia, albedo and emissivity of building envelope, street aspect ratio, plan density	Neighborhood	Simulation (TEB)	One year	*T*: −1.21 to +0.34 K
Allegrini and Carmeliet 2018	Zürich, Switzerland; Temperate maritime	Building configuration of district	District	Simulation (ENVI-met)	An extreme hot day	WS: −1.7 to −0.1 m/s; *T*: −0.7 to +1.2 K
Bueno et al. 2013	Basel, Switzerland; Toulouse, France; Temperate maritime	Thermal properties of construction materials	City	Simulation (UWG)	1 year	*T*: +2.4 to +3.6 K
Tsoka 2017	Thessaloniki, Greece; Mediterranean	Cooling materials of building (emissivity and albedo), district aspect ratio	District	Simulation (ENVI-met)	A typical summer day under clear sky condition	*T*: −0.5 to −0.7 K
Allegrini and Carmeliet 2017	Zürich, Switzerland; Temperate maritime	Building height topologies of district	District	Simulation (OpenFOAM)	A selected hour	*T*: +1.5 to +2.5 K
Bourbia and Boucheriba 2010	Constantine, Algeria; Mediterranean	Street height/width ratio, sky view factor	District	On-site monitoring	1 month	*T*: +3 to +6 K
Merlier et al. 2019a	Lyon, France; Continental temperate marine	Building configuration of district	District	Simulation (SOLENE-microclimat)	2 selected days	*T*: +0.1 to +2.7 K
Dimoudi et al. 2013	Serres, Greece; Mediterranean	District geometry and street configuration	District	On-site monitoring	1 month	WS: −67% to −75%; *T*: +5 to +5.5 K in afternoon and night, −7 K in morning
Hang and Li 2010	Zürich, Switzerland; Temperate maritime	District geometry and albedo	District	Simulation (CFD)	A summer afternoon	*T*: +1 K
Xie et al. 2020	Reading, UK; Temperate maritime	Building form	Neighborhood	On-site monitoring	1 year	*T*: +0.27 to +0.73 K
Shen et al. 2021	Shenzhen, China; Subtropical monsoon	Building height, aspect ratio, compactness ratio, number of footprint vertices	District	Simulation (UWG)	1 week	*T*: +5.9 K
Ignatius et al. 2015	Singapore; Tropical rainforest	Floor area ratio, gross site coverage, open space ratio, number of stories, sky view factor	District	Simulation (STEVE)	—	*T*: −1.3 K

Note: *T*, WS and RH refer to the air temperature, wind speed and relative humidity, respectively.

monitored weather data collected from ten rural stations and seven urban stations in Beijing were used for the UHI effect estimation. It can be observed that most existing studies just use the monitored meteorological data with UHI effect to simulate the building performance of the reference building, while the impacts of building design itself on the local microclimate and the impacts of local microclimate on different building design are always ignored (Allegrini et al. 2012; Yassin 2013; Zinzi et al. 2018).

Though considerable work has been done to investigate the impacts of building design on local microclimate and the impacts of local microclimate on building performance

Table 2 Representative studies on the impacts of local microclimate on building performance

Reference	Location and climate	Variation of microclimate	Building type	Quantification method	Period	Impacts on building performance
Ge et al. 2023	Xi'an, China; Temperate continental	*T*: −0.8K; WS: +0.2 to 0.8 m/s	District in residential blocks	Simulation (EnergyPlus)	1 month	HL: +0.7 to +1.6 kWh/m^2
Wang et al. 2024	Chicago, USA; Humid continental	*T*: +5.5 K (maximum)	A medium office building	Simulation (coupling VCWG and EnergyPlus)	1 month	CL: −8.8 % to + 17.5 %
Diz-Mellado et al. 2023	Seville, Spain; Mediterranean	*T*: −4 to 14.4 K	Three dwellings with an interior courtyard	Simulation (HULC)	Warmer months under cooling conditions	CL: −18% to −8%
Xie et al. 2020	Reading, UK; Temperate maritime	*T*: −0.27 to +0.73 K	A five-storey faculty building	Simulation (IES-VE)	1 year	HL: −10.8%; night ventilation cooling potential: +26% to +31%
Mosteiro-Romero et al. 2020	Zürich, Switzerland; Temperate maritime	*T*: −0.7 to +1.2 K; WS: −1.7 to −0.1 m/s	Real buildings in a district	Simulation (City Energy Analyst)	An extreme hot day	CL: +5%
Shen et al. 2021	Shenzhen, China; Subtropical monsoon	*T*: +5.9 K; RH: −26.3%	4 DOE reference buildings	Classical equations	1 week	Cooling degree days: +12.60%; heating degree days: −11.92%
Ignatius et al. 2015	Singapore; Tropical rainforest	*T*: −1.3 K	District	Simulation (STEVE)	—	CL: −4%
Zinzi et al. 2018	Rome, Italy; Mediterranean	*T*: +2.8 K in summer, +1 K in winter	A residential building & an office building	Simulation (TRNSYS)	3 years	CL: +53 to +74%; HL: −18 to −21%
Guattari et al. 2018	Rome, Italy; Mediterranean	*T*: +2 K in summer, +1.6 K in winter	A detached building	Simulation (TRNSYS)	1 year	CL: +30%; HL: -11%
Palme et al. 2017	4 South American Pacific coastal cities; Tropical rainforest & desert	*T*: −1.15 to +0.59 K at night, +0.15 to +4.87 K in daytime	Single building	Simulation (TRNSYS)	A summer week	CL: +15 to +200%
Paolini et al. 2017	Milan, Italy; Mediterranean	*T*: +1.1 K; *H*: −0.67 g/kg	A residential building	Simulation (WUFI Plus)	6 years	HL: −12% to −16%; CL: +39% to +41%; dehumidification load: −74% to −78%; T: +1.4+1.5 K
Salvati et al. 2017	Barcelona, Spain; Mediterranean	*T*: +1.7 K in summer, +2.8 K in winter	A residential building	Simulation (EnergyPlus)	Two summer days	Sensible CL: +18% to +28%
Cui et al. 2017	Beijing, China; Temperate monsoon	*T*: +2.5 K in summer daytime, +8 K in winter nighttime	A seven-storey office building	Simulation (DeST)	1 year	CL: +11%; HL: −16%
Shi et al. 2019	Hong Kong, China; Subtropical monsoon	*T*: +2.4 K; *H*: +0.68g/kg	A high-rise residential building	Simulation (DeST)	9 years	Sensible CL: +100%; latent CL: +96%
Merlier et al. 2019b	Lyon, France; Continental temperate marine	*T*: +1.7 to +2.8 K	A monozone building	Simulation (BuildSysPro)	Two selected days	HL: −5% to −7%; CL: +23 to +100%

Note: *T*, RH, *H* and WS refer to the air temperature, relative humidity, absolute humidity and wind speed, respectively; HL and CL refer to heating load and cooling load, respectively.

(Mutani and Fiermonte 2016; Ali-Toudert and Böttcher 2018, Allegrini and Carmeliet 2018), only a few papers (6 papers (Ignatius et al. 2015; Mosteiro-Romero et al. 2020; Xie et al. 2020; Shen et al. 2021; Diz-Mellado et al. 2023; Wang et al. 2024) among the reviewed 43 papers) study the mutual impacts between building design and local microclimate. For instance, Wang et al. (2024) established an interactive indoor-outdoor building energy modeling method to enhance the predictions of urban microclimates and building energy demands by coupling an urban physics model with a physics-based building energy model. Xie et al. (2020) conducted the one-year monitoring of the local

microclimate surrounding four different forms of building in Reading, UK. These meteorological data with local microclimate effect was further used to estimate the building performance of reference building. Mosteiro-Romero et al. (2020) utilized ENVI-met to simulate the local microclimate due to the presence of the district, and utilized City Energy Analyst to simulate the district's energy demands considering the local microclimate effect on two hot days in Zurich, Switzerland. Though these studies consider both impacts of building design on local microclimate and impacts of local microclimate on building performance, the mutual impacts between them are not addressed thoroughly. The research gaps can still be observed in the existing mutual impacts studies. Firstly, the existing studies mainly investigate the impacts of district design rather than individual building design on the local microclimate (Allegrini and Carmeliet 2018; Merlier et al. 2019a; Mosteiro-Romero et al. 2020). These district design parameters related to district density and district geometry (e.g., plan density, street height/width ratio and sky view factor) are useless in individual building design due to the existing surroundings. Though these research outcomes can be adopted in district/urban planning, they are insufficient to support the building design. Secondly, several existing studies investigate the impacts of building design on the local microclimate by monitoring or simulating the local microclimate using limited samples (Allegrini and Carmeliet 2018; Merlier et al. 2019a; Mosteiro-Romero et al. 2020). However, there is still a lack of comprehensive understanding of the major influential building parameters on both building performance and local microclimate to support the building design considering the mutual impacts. Thirdly, the simplified geometry model of the neighborhood/district used in existing studies ignores the real terrain (Allegrini et al. 2015; Allegrini and Carmeliet 2018; Merlier et al. 2019a; Mosteiro-Romero et al. 2020), which may increase the bias of estimation on the impacts between buildings and local microclimate (Allen-Dumas et al. 2022). Fourthly, the impacts of building design variations on the local microclimate and the impacts of local microclimate on building performance under different building designs are ignored when assessing the building energy performance (Lee and Jeong 2017; Merlier et al. 2019a; Mosteiro-Romero et al. 2020; Xie et al. 2020).

Nowadays, the development or renewal of individual buildings in the existing district is a common practice compared with the full development of entire districts due to the limited available spaces in developed and high-density cities. However, very few papers (2 papers (Merlier et al. 2019b; Xie et al. 2020) among the reviewed 37 papers) concern the impact of individual building design on local microclimate. The results show that four buildings with different morphologies in the same district can lead to the increase of local air temperature by 0.27–0.73 K (Xie et al. 2020). Therefore, a new design perspective is needed for developing individual buildings in existing high-density urban areas.

In this study, a comprehensive and systematic analysis is therefore conducted to investigate the mutual impacts between new individual building design and the local microclimate considering the interaction between them in high-density cities, and to identify the major influential building parameters on both local microclimate (e.g., air temperature, wind velocity, and pedestrian thermal discomfort) and building energy performance in subtropical urban area. The mutual impacts are assessed based on 200 sets of building and microclimate simulations using different building designs. Advanced spatial analysis techniques based on GIS (geographic information systems) are adopted for high-resolution 3-dimentional (3D) microclimate simulation and building performance simulation. Based on the impact analysis, the major influential building parameters on both the local microclimate and building energy performance are finally identified by a global sensitivity analysis. The significance of this study is that strong mutual impacts between the new building design and urban local microclimate are demonstrated. It is necessary to consider the mutual impacts in the design of new buildings because the correlations between the parameters and the performances (i.e., building energy performance and pedestrian thermal discomfort) are significantly different. The outcomes of this study can provide the basis for the consideration of mutual impacts between buildings and local microclimate in new building or rebuilding design at the early stage to enhance both building energy performance and local microclimate.

2 Overall research methodology and procedure

2.1 Overview of the research case

A new student dormitory building to be developed in Kowloon, Hong Kong is used as the case to investigate the mutual impacts between new individual building design and local microclimate in high-density city in this study. Figure 1 shows the aerial view of the study area and the location of the new building. The building will be located on a hillside nearby the Tat Hong Avenue, Kowloon, which is a dense and central urban area in Hong Kong. The maximum land area available for the new building is 170 m × 125 m. Hong Kong is characterized by high-density and high-rise development. The climate in Hong Kong is subtropical monsoon. In summer, the average air temperature is approximately 28 °C and the average relative humidity is more than 80% (Wang et al. 2018), while in winter, the

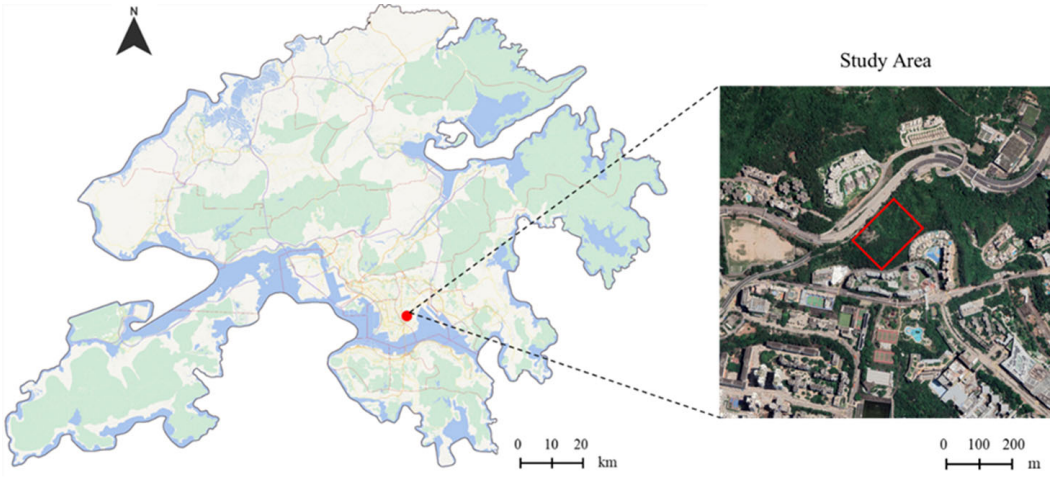

Fig. 1 Aerial view of the study area and the location of the new building

ambient temperature below 10 °C is not common in urban areas (Li et al. 2018). The prevailing wind direction is from the east.

2.2 Building parameters concerned

A total of 6 building parameters affecting both building performance and local microclimate are considered in the mutual impact assessment and sensitivity analysis in this study as listed in Table 3. They can be classified into two main categories, i.e., building morphology and building thermal characteristics. The building morphology parameters include building height, building orientation, and building aspect ratio. The building thermal characteristics parameters include the overall heat transfer coefficient of building envelope, emissivity of wall, and heat rejection of air-conditioners. The variation ranges of the parameters are set as wide as possible by referring to the requirements in related design codes (Buildings Department 2014; GB/T 51350 2019; Inanici and Demirbilek 2000) and the settings in previous research (Inanici and Demirbilek 2000; Allegrini and Carmeliet 2017; Ali-Toudert and Böttcher 2018).

Building aspect ratio (Mohammad et al. 2015; Shen et al. 2021), building height (Bueno et al. 2013; Ignatius et al. 2015; Allegrini and Carmeliet 2017; Shen et al. 2021), orientation (Ali-Toudert and Mayer 2006; Chen et al. 2017), emissivity (Hang and Li 2010; Bueno et al. 2013; Mutani and Fiermonte 2016; Tsoka 2017; Ali-Toudert and Böttcher 2018), building height (Bueno et al. 2013; Ignatius et al. 2015; Allegrini and Carmeliet 2017; Shen et al. 2021) and heat transfer coefficient (Ali-Toudert and Böttcher 2018) are the key influential parameters of building design affecting local microclimate, which are widely investigated in previous studies as shown in Table 1. It is worth noticing that the heat rejection of air-conditioners, as a major source of anthropogenic heat particularly in cooling-dominated regions (Mao et al. 2018), has not been investigated in previous studies on local microclimate but included in this study. Existing related research only focuses on the airflow and temperature near the condensing units of air-conditioners, to determine their optimum placement for enhanced system coefficient of performance (Chow et al. 2002; Avara and Daneshgar 2008; Liu et al. 2019). Though the district design parameters (e.g., district density (Bueno et al. 2013; Mohammad et al. 2013; Ignatius et al. 2015; Ali-Toudert and Böttcher 2018; Shen et al. 2021), district morphology (Dimoudi et al. 2013; Allegrini and Carmeliet 2017; Chen et al. 2017; Allegrini and Carmeliet 2018; Mosteiro-Romero

Table 3 Building parameters concerned in this study

Category	Parameter	Range	Unit
Building morphology	Building height	6–200	m
	Building orientation	0 to 360	(°)
	Building aspect ratio	1:1, 1.2:1, 1.4:1, 1.5:1, 2:1, 3:1, 4:1, 5:1, 6:1, 7:1, 8:1, 9:1	—
Building thermal characteristics	Overall heat transfer coefficient of building envelope	1.1–14.0	W/(m^2·K)
	Emissivity of wall	0–1	—
	Heat rejection of air-conditioners	75–150	W/m^2

et al. 2020), street height/width ratio (Bueno et al. 2013; Theeuwes et al. 2014; Tsoka 2017; Ali-Toudert and Böttcher 2018; Bourbia and Boucheriba 2020) and sky view factor (Bourbia and Boucheriba 2010; Ignatius et al. 2015)) are widely concerned in previous microclimate studies, they are not considered in this study because they are not the building design parameters affecting the building performance directly. In the research scenario with existing surroundings, the district design parameters which reflect the relationship of buildings can be determined by the three selected building morphology parameters.

2.3 The procedure and methods

In this study, the mutual impacts between individual building design and local microclimate are investigated and a global sensitivity analysis is conducted by varying the building parameters simultaneously. The detailed procedure is illustrated in Figure 2. Firstly, 200 scenarios of building design are generated using Latin hypercube sampling method (Bourbia and Boucheriba 2010) according to the ranges of the main building parameters concerned (as shown in Figure 3). Secondly, the local microclimate under each scenario of building design is simulated using Fluent based on the district 3D geometry model generated based on GIS under the hottest hour on the summer typical design day. 3D steady Reynolds-averaged Navier-Stokes (RANS) CFD simulations of incompressible flow are performed using RNG k-ε turbulent model. The typical meteorological year (TMY) weather data is used as the weather data input for the local microclimate simulation in this study. After generating the microclimate effect for each building design under the hottest hour, the microclimate effect is added to each hour of the summer typical design day (including 24 hours). Then the building energy performance for each scenario of building design is simulated for the summer typical design day (including 24 hours) considering the microclimate effect. using EnergyPlus. The weather data generated considering the microclimate impacts is used as the weather data input. Fourthly, the values of performance indexes under different scenarios are calculated based on the simulation results of local microclimate and building energy performance. The performance indexes include: (i). the average difference between pedestrian-level (i.e., 3.0 m away from the building and 1.5m height in this study) air temperatures of the district with and without the new building (local air temperature difference in short in the rest of this paper); (ii). the average difference between pedestrian-level wind velocities of the district with and without the new building (local wind velocity difference in

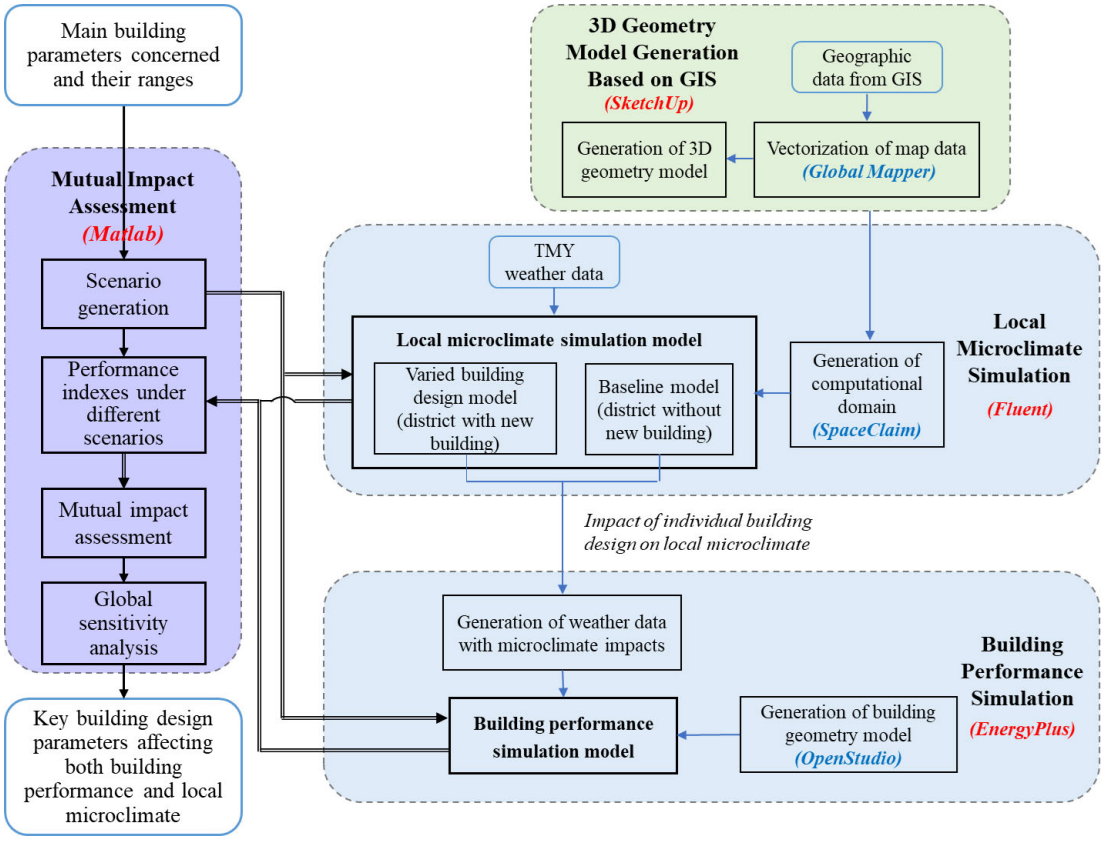

Fig. 2 Outline of the overall research methodology and procedure

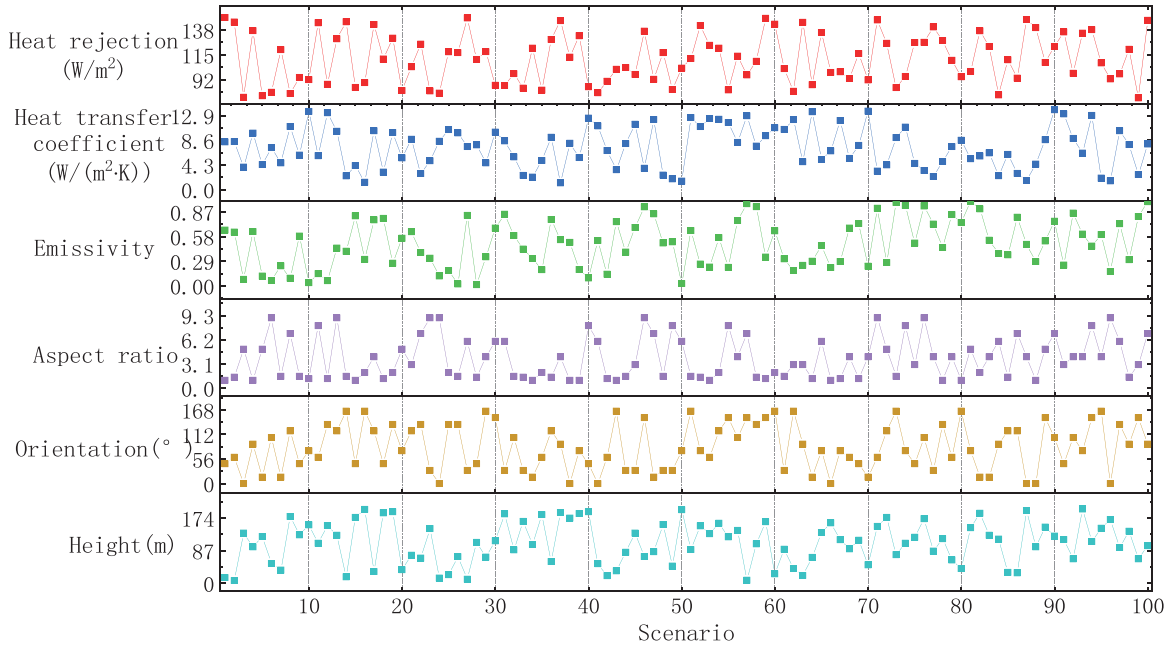

(a) Scenario 1 to Scenario 100

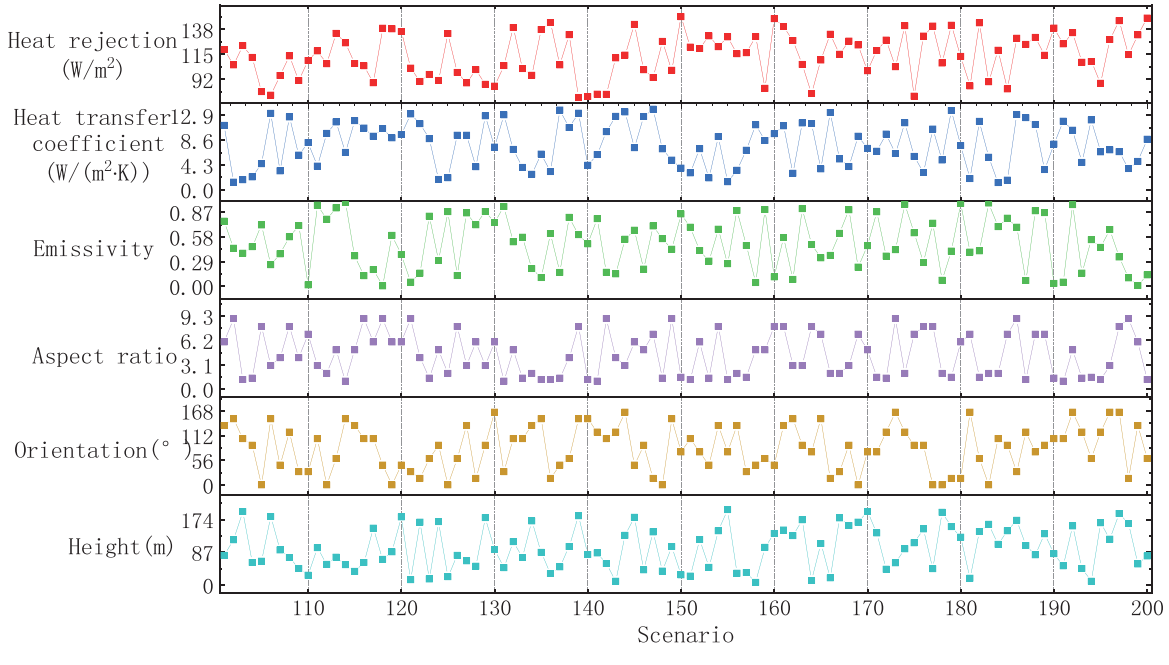

(b) Scenario 101 to Scenario 200

Fig. 3 200 scenarios generated by Latin hypercube sampling method

short); (iii). the pedestrian thermal discomfort degree of the district considering local microclimate impacts (pedestrian thermal discomfort degree in short, D_{discom}); (iv). the building energy consumptions considering the interaction with local microclimate per area (the building energy consumption in short). Fifthly, mutual impact assessment is performed in Matlab based on the calculated performance indexes. The mutual impact assessment includes the analysis on the impacts of building design on local microclimate (e.g., air temperature, wind velocity, and pedestrian thermal discomfort), and the impacts of local microclimate on building energy performance. Based on the mutual impact assessment, the major influential building parameters on both the local microclimate and building energy performance are finally identified through a global sensitivity analysis.

3 High-resolution 3D microclimate simulation and building simulation using advanced GIS-based spatial analysis techniques

3.1 High-resolution 3D microclimate simulation model based on GIS

The investigation on the mutual impacts of individual building design and local microclimate needs very detailed and accurate geographic information. In this study, 3D structural geological model of high resolution is adopted based on advanced GIS spatial analysis technique for subsequent high-accuracy microclimate simulations. The CFD simulations of the 200 design scenarios are conducted under the most unfavorable weather condition (the hottest hour) of the summer typical design day with the prevailing wind condition in order to assist the evaluation of the design performance and significantly reduce the computing cost. The development of high-resolution 3D microclimate simulation model involves: the generation of computational domain based on GIS, grid discretization, and the development of the microclimate simulation model, which are introduced in detail as below.

3.1.1 Generation of computational domain

The 3D computational domain is generated using advanced spatial analysis techniques based on GIS. GIS is a system which can store, visualize, analyze, and interpret geographic data. The geographic data includes the descriptive information of the geographic features, such as the altitude/elevation, the widths of roads, and the locations and dimensions of buildings, which are necessary for generating the computational domain for CFD (computational fluid dynamics) simulation (Kong et al. 2017). The utilization of GIS allows to account for the complexity of the urban structure and the specific surface characteristics on a fine spatial scale (Back et al. 2023). It can not only simplify the process of generating the computational domain while ensuring the accuracy of microclimate simulation, but also benefit the spatial analysis by reloading the simulation data back to GIS.

The generation of computational domain includes two main steps. Firstly, the geographic data of the target district is collected from Google Map. Secondly, the captured geographic data is vectorized and converted using Global Mapper to generate the 3D geometry model of the district, which contains the landforms, buildings and roads. Figure 4 shows the 3D geometry model of the target district in this study, which is a 1,000 m × 1,000 m urban area in Kowloon, Hong Kong. Based on the developed district 3D geometry model, the whole computational domain is generated using SpaceClaim. The dimension of the entire computational domain for microclimate simulation as shown in Figure 5 is determined to be 8,000 m × 4,500 m × 2,100 m for fully developed flow according to the CFD simulation guidelines and previous research (Tominaga et al. 2005; Tominaga et al. 2008).

3.1.2 Grid discretization

Grid discretization is performed using the software Meshing. The unstructured grid is used in this study in view of the complicated geometry of the target district. The grid

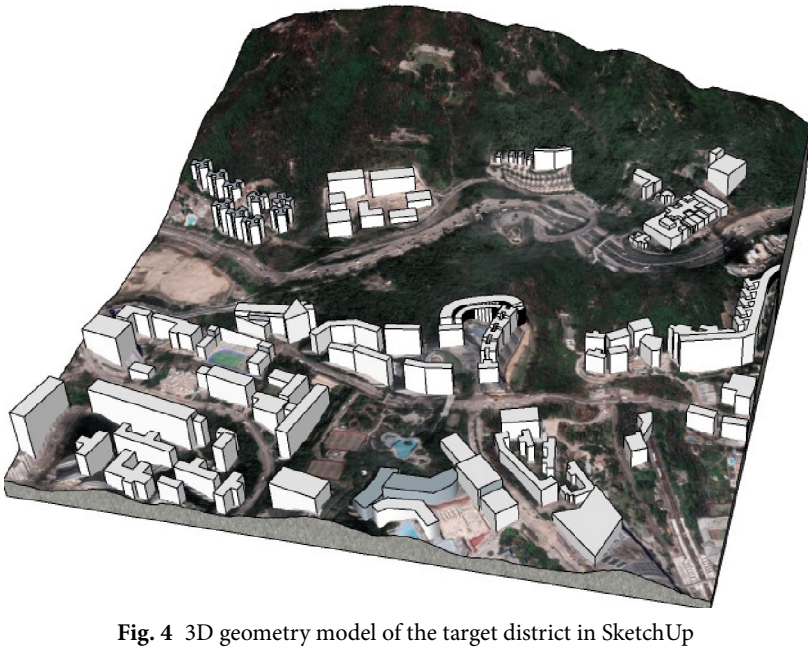

Fig. 4 3D geometry model of the target district in SketchUp

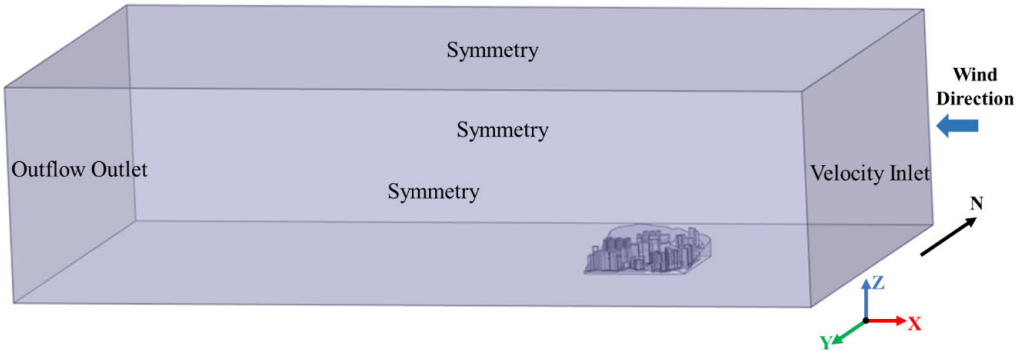

Fig. 5 3D computational domain in SpaceClaim

independence verification is performed based on three grid systems to find the proper grid resolution, including a coarse grid system, a basic grid system, and a fine grid system. The basic grid system is finally adopted and the grid number in the 200 cases of microclimate simulations ranges from 8.225 to 31.071 million. Local grid refinement is implemented near the wall of the buildings and the ground, while coarser mesh is for far field.

3.1.3 Development of high-resolution 3D microclimate simulation model

In this study, two types of 3D microclimate simulation models are developed using Fluent based on the generated computational domain and mesh in order to investigate the impacts of new building development on the local microclimate. One is the 3D simulation model of the target district without the new building, which is regarded as the baseline model for comparison. The other one is the microclimate simulation models of the target district with different designs of individual building. The impacts of the individual building design on the local microclimate are quantified by: (i). the local air temperatures difference; (ii). the local wind velocity difference; (iii). the pedestrian thermal discomfort degree (D_{discom}). *As* its name implies, D_{discom} is defined to assess the degree of outdoor thermal discomfort at the pedestrian level. A higher absolute value means a higher degree of thermal discomfort. It is calculated based on the widely-used outdoor thermal comfort index PET (Potchter et al. 2018), as shown in Equations (1)–(2). PET_{n} is the neutral physiological equivalent temperature, which is set to 28 °C in this study (Ng and Cheng 2012). PET_{ave} is the average PET of male (PET_{male}) and female ($\text{PET}_{\text{female}}$).

$$D_{\text{discom}} = \text{PET}_{\text{ave}} - \text{PET}_{\text{n}} \tag{1}$$

$$\text{PET}_{\text{ave}} = \left(\text{PET}_{\text{male}} + \text{PET}_{\text{female}}\right)/2 \tag{2}$$

3D steady Reynolds-averaged Navier-Stokes (RANS) CFD simulations of incompressible flow are performed using RNG k-ε turbulent model due to its high accuracy (Tominaga et al. 2005). For the near-wall treatment, scalable wall functions with no-slip boundary condition are adopted considering the compromise between simulation accuracy and computing cost. Radiation with discrete ordinates (DO) model is adopted in the calculation. As the prevailing wind in Hong Kong is from the east, the right surface of the computational domain is determined as the velocity inlet as shown in Figure 5. The vertical velocity profile U_z, the turbulent kinetic energy k_z, and the turbulence dissipation ε_z are calculated according to the AIJ's benchmark tests, as shown in Equations (3)–(7) (Tominaga et al. 2008; Lin et al. 2014; Ding and Lam 2019). The downstream boundary is defined as outflow. The lateral and upper surfaces of the computational domain are set as the symmetry boundary conditions. The surfaces of buildings and the ground are set as the no-slip wall boundary conditions. The boundary conditions (shown in Figure 5) are set according to the CFD simulation guidelines and previous research (Franke et al. 2007; Martilli et al. 2007; Tominaga et al. 2008; Chen et al. 2017; Ding and Lam 2019). The boundary conditions and parameter settings of the CFD model are validated by comparing the numerical modeling results with the wind tunnel test data of Case E wind tunnel experiment made by Architecture Institute of Japan (AIJ) (Tominaga et al. 2004) in order to ensure the fidelity of the CFD simulation results. The wind tunnel experiment area of Case E is an actual urban area in the Niigata city of Japan, the configuration of which is similar to our study area. The CFD simulations is performed using Fluent (2019R3) in a server with an AMD EPYC 7T83 CPU at 3.40 GHz and Windows 10 Enterprise 64-bit OS. The computational time for each CFD simulation is about 1–2 hours.

$$U_z = U_s \cdot \left(\frac{z}{z_s}\right)^{\alpha} \tag{3}$$

$$k_z = 1.5 \cdot \left(I_z \cdot U_z\right)^2 \tag{4}$$

$$I_z = 0.39 \cdot \left(\frac{z}{10}\right)^{-\alpha} \quad (5)$$

$$\varepsilon_z = C_\mu^{0.75} \cdot k_z^{1.5} / l_z \quad (6)$$

$$l_z = 100 \cdot \left(\frac{z}{30}\right)^{0.5} \quad (7)$$

where, z is the vertical coordinate of the calculation point in the computational domain. U_s is the velocity at the reference height, which is set to 2.639 m/s in this study. z_s is the reference height, which is set to 62 m in this study. α is the power-law exponent, which is set to 0.39 according to the terrain category. I_z is the turbulent intensity. C_μ is the model constant, the value of which is 0.09. l_z is the turbulence integral length.

3.2 Building simulation model

The impacts of the local microclimate on the building energy performance considering the interaction between them are quantified by: the building energy consumption, which consists of the energy consumption for cooling, lighting and other equipment per area of the building in subtropical region on summer typical design day including 24 hours. The weather data which considers the impacts of local microclimate is used for the building energy performance simulation. As introduced in Section 2.3, the building simulation model is developed using EnergyPlus. Figure 6 shows an example of the building geometry model for building performance simulation.

The operating time of the building and the air-conditioning system is 0:00–24:00 on all days. The water-cooled electric chillers are adopted for the cooling system.

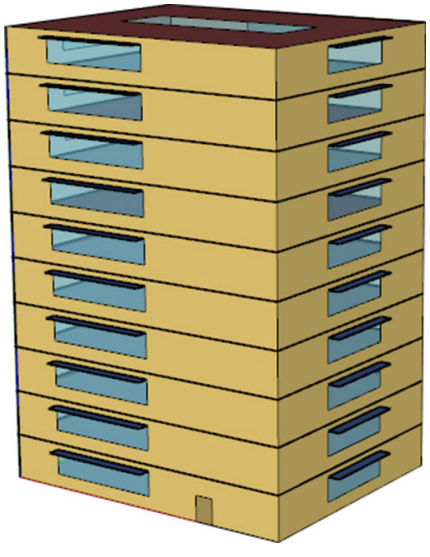

Fig. 6 An example of the building geometry model for building performance simulation

The overall coefficient of performance of air-conditioning system is determined as 4. The control logics of the air-conditioning and lighting systems in the model are set to maximize the use of natural ventilation and daylight (Zhao et al. 2022). The schedules of the occupancy rate and the utilization rates of electric lights, equipment and HVAC system are set according to Table 4. Humidity control is also considered in the simulation model. The setpoint of relative humidity is set at 60% (Zhao et al. 2022).

The internal settings and the settings of the parameters not under investigation in the simulation model are determined as shown in Table 5. The standard floor height is set as 3 m, and the ground floor height can be 3, 4, or 5 m. The building height is increased by increasing the floor number and varying the ground floor height. The dimension of each building design scenario is determined by Latin hypercube sampling method, which has the maximum floor area under the sampled orientation and aspect ratio in the design area available for the new building (170 m × 125 m) and has the sampled height. The dimension can be modified by controlling the coordinate settings.

As a large number of building performance simulations are required for a comprehensive mutual impact analysis between the new building and the local microclimate, jEplus is adopted to achieve the automatic process of numerous building performance simulations. jEplus can automatically modify the parameter values (i.e., the six parameters listed in Table 3) in building simulation model according to the generated scenarios and call EnergyPlus to perform the simulation.

Table 4 Daily schedule of occupancy rate, electric light utilization rate, electric equipment utilization rate and HVAC system utilization rate

Operating Time	Occupancy rate	Electric light utilization rate	Electric equipment utilization rate	HVAC system utilization rate
0:00–1:00	0.95	0.30	0.30	1
1:00–2:00	0.95	0.20	0.20	1
2:00–5:00	0.95	0.10	0.10	1
5:00–6:00	0.95	0.10	0.20	1
6:00–7:00	0.95	0.70	0.40	1
7:00–8:00	0.95	0.40	0.50	1
8:00–9:00	0.90	0.60	0.40	1
9:00–10:00	0.30	0.60	0.40	1
10:00–17:00	0.30	0.36	0.25	1
17:00–19:00	0.50	0.50	0.60	1
19:00–20:00	0.95	0.80	0.80	1
20:00–23:00	0.95	0.80	0.90	1
23:00–24:00	0.95	0.80	0.50	1

Table 5 The internal settings and the settings of the parameters not under investigation in the simulation model

Parameter	Value	Unit
Window to wall ratio	0.25	—
Wall specific heat	920	J/(kg·K)
Wall thermal absorptance	0.9	—
Wall solar absorptance	0.7	—
Wall visible absorptance	0.7	—
Roof specific heat	920	J/(kg·K)
Roof thermal absorptance	0.9	—
Roof solar absorptance	0.7	—
Roof visible absorptance	0.7	—
Ground slab specific heat	920	J/(kg·K)
Ground thermal absorptance	0.9	—
Window SHGC	0.15	W/(m²·K)
Window visible light transmittance	0.61	—
Infiltration air mass flowrate coefficient	1	h^{-1}
Outdoor airflow rate	0.00944	m³/(person·s)
Indoor setpoint temperature for cooling	25.5	°C
Overhang tilt angle	90	(°)
Sensible heat recovery effectiveness	0.7	—
Latent heat recovery effectiveness	0.65	—
Occupancy	4	m²/person
People load	108	W/person
Lighting load	10	W/m²
Electric equipment load	7.6	W/m²

4 Results of the mutual impact assessment

4.1 Impacts of building design on local microclimate

The distributions of local air temperature differences under the 200 scenarios on the three building morphology parameters are shown in Figure 7(a) and on the three building thermal characteristics parameters are shown in Figure 7(b). It can be seen that the development of a new building in an existing district will not always lead to an increase in the local air temperature surrounding the building. Different building designs bring impacts of varying degrees on the local air temperature. In this research case, the local air temperature difference varies between −0.60 K and +1.17 K under different building design scenarios. Among them, 49% of the scenarios have a decrease in the local air temperature, and 50% of the scenarios have a temperature increase higher than 0.40 K. The air temperature distributions under different target buildings in planning are significantly different. Take Scenario 87 (shown in Figure 8(a)) and 37 (shown in Figure 8(b)) as examples, when the building orientation increases from 0° (Scenario 87) to 90° (Scenario 37) and other 5 design variables vary by a little (0–5% of their varying ranges), the local air temperature increases by 0.48 K. This is because when the control strategy adopted in the design building maximizes the use of natural ventilation, an orientation aligning with the windward direction can promote the wind flow and thus reduce the local air temperature, otherwise, the reverse.

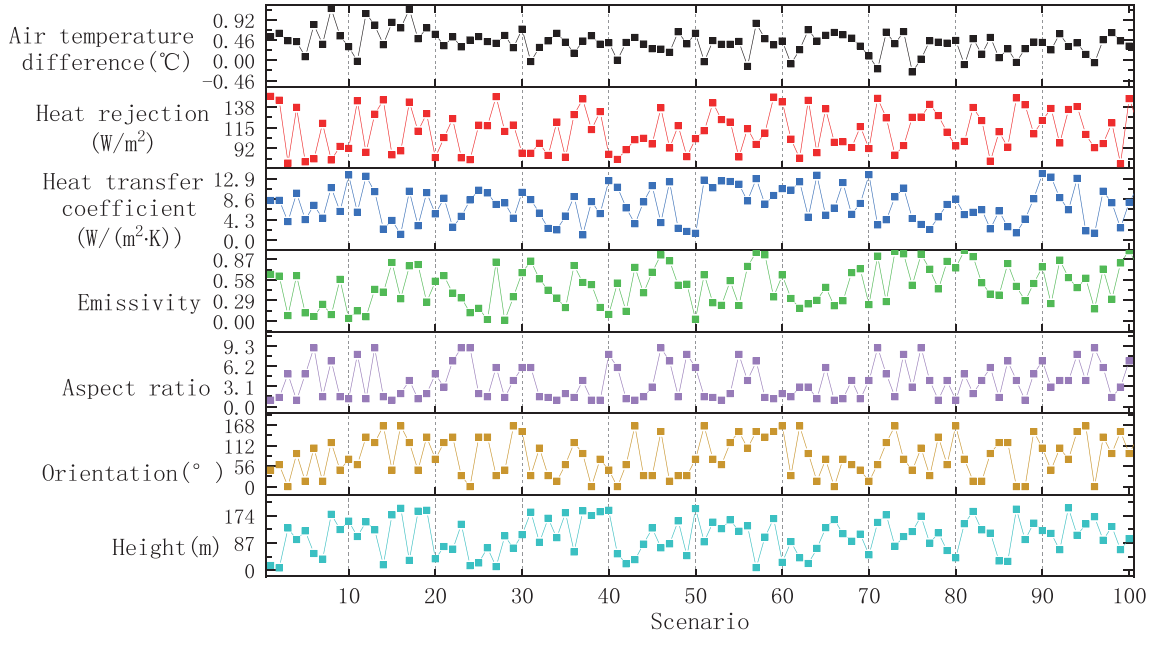

(a) Scenario 1 to Scenario 100

Fig. 7 Local air temperature differences between with and without the new building under different scenarios

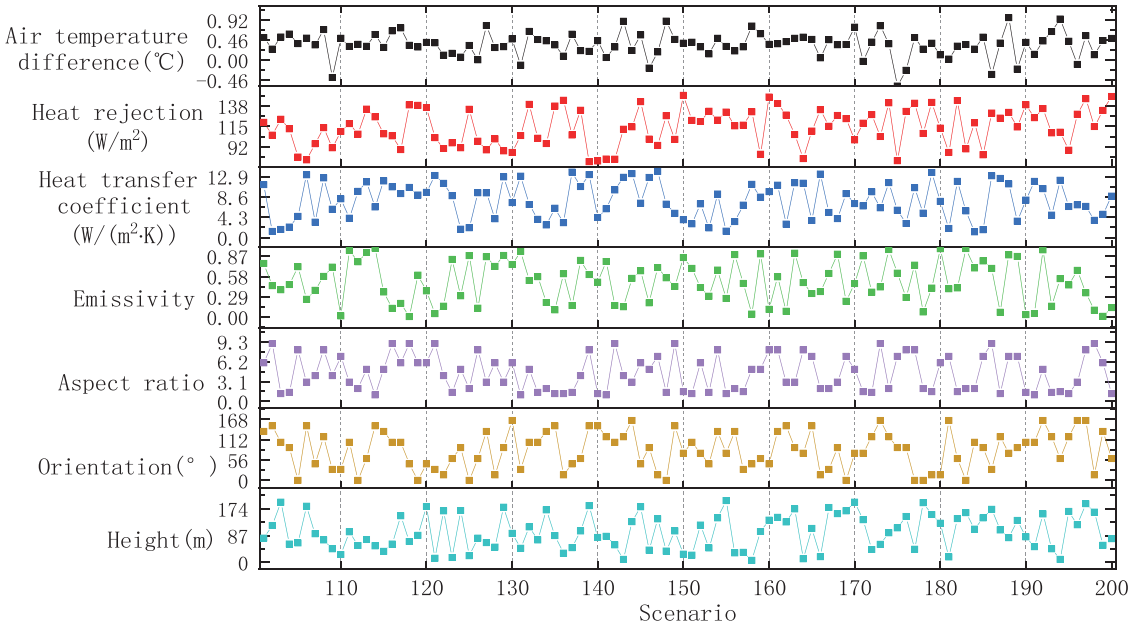

(b) Scenario 101 to Scenario 200

Fig. 7 Local air temperature differences between with and without the new building under different scenarios (Continued)

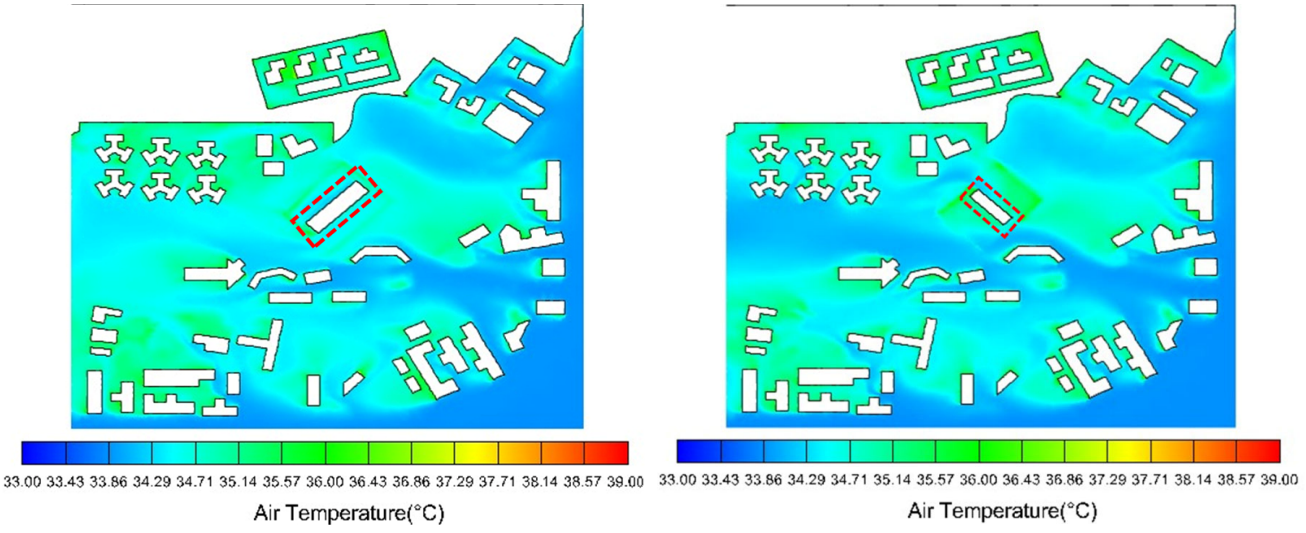

(a) Scenario 87 (b) Scenario 37

Fig. 8 Air temperature distributions at z = 1.5 m of magnified view of study area

The results of local wind velocity differences under the 200 building design scenarios are shown in Figure 9(a) and Figure 9(b). It can be seen that different designs of a new building can lead to an increase or decrease in the local wind velocity surrounding the building. The local wind velocity difference between with and without the new building varies from −0.95 m/s to +4.51 m/s under the 200 design scenarios. In nearly half of the scenarios, the local wind velocity is increased and the wind velocity difference falls within a range between 0.01 m/s and 0.95 m/s. The average wind velocity difference under all of the scenarios is 0.15 m/s. The wind velocity distributions under different building design are absolutely different. It can be observed from Figure 10(a) (Scenario 23) and Figure 10(b) (Scenario 33) that the building aspect ratio has considerable impacts on the local wind velocity. The increase of the aspect ratio from 1.4:1 (Scenario 33) to 9:1 (Scenario 23) can lead to 0.57 m/s of velocity increase because the flow past a building which seems like a flat plate can promote the ventilation around it.

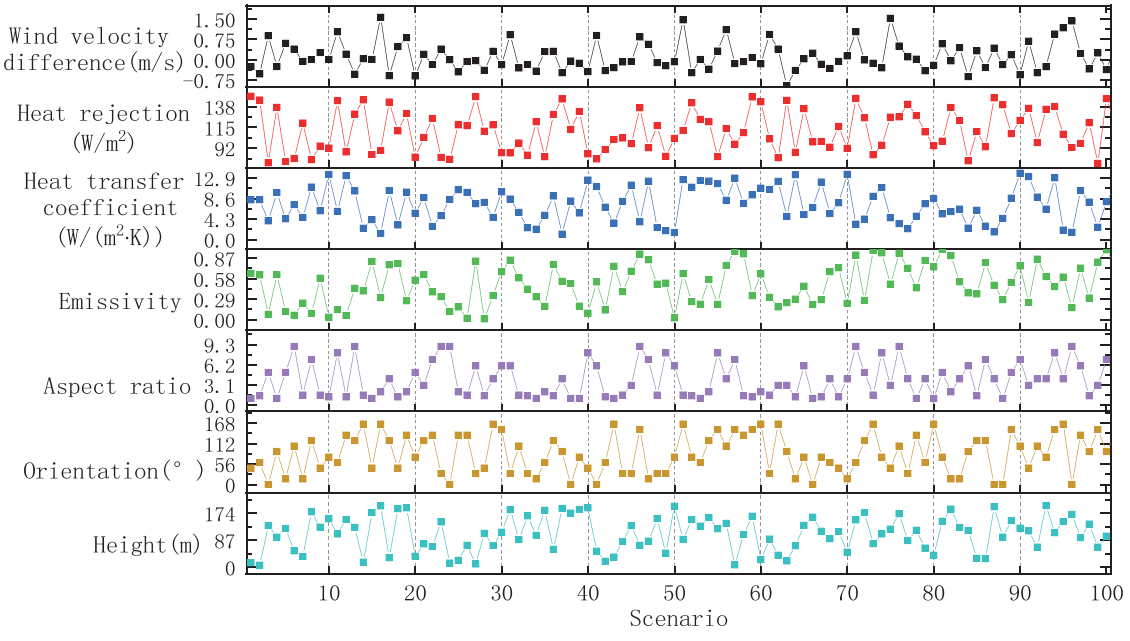

(a) Scenario 1 to Scenario 100

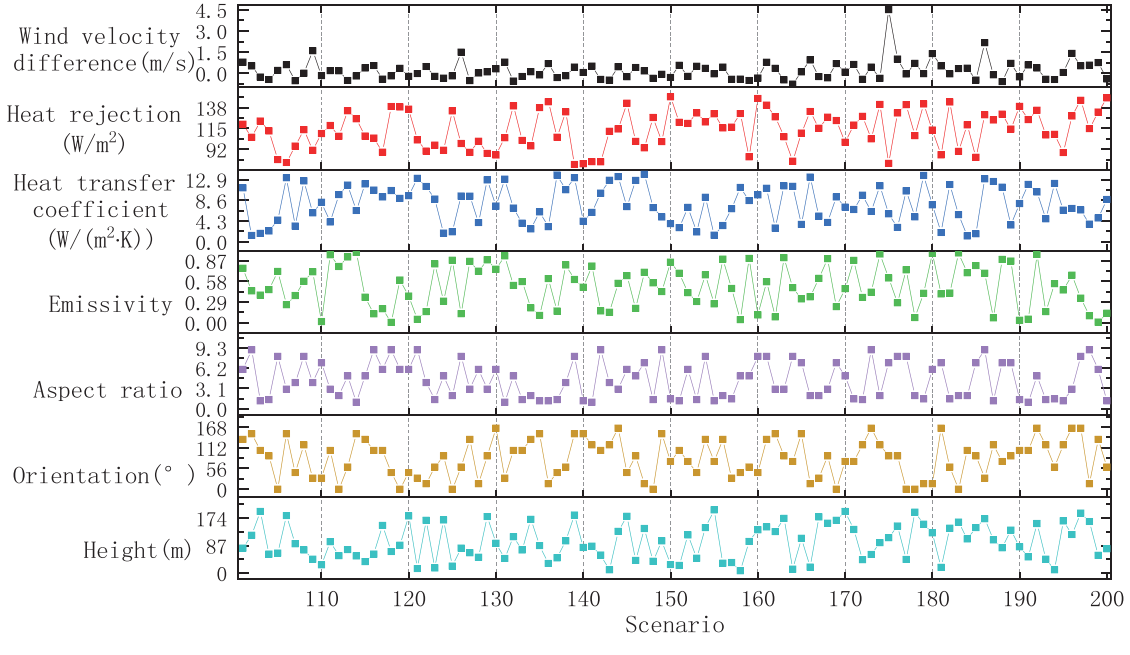

(b) Scenario 101 to Scenario 200

Fig. 9 Local wind velocity differences between with and without the new building under different scenarios

The pedestrian thermal discomfort degrees under the 200 building design scenarios are shown in Figure 11. It can be seen that the pedestrian thermal discomfort degree varies from 13.75 to 22.65 °C under different building design scenarios, corresponding to the thermal perception from hot to very hot. 95.5% of the scenarios have a high pedestrian thermal discomfort degree higher than 18 °C. The average pedestrian thermal discomfort degree is around 20.61 °C. Figure 12 shows the pedestrian thermal discomfort degrees of the district under the typical scenarios of building design. It can be seen that the one-variable-dominated variation (other 5 building design variables setting as the same or varying by a little) can lead to the changes of pedestrian thermal discomfort degree in the range of −1.45 to 3.90 °C. The increase of building height from 65 m (Scenario 92) to 141m (Scenario 56) can dominate the

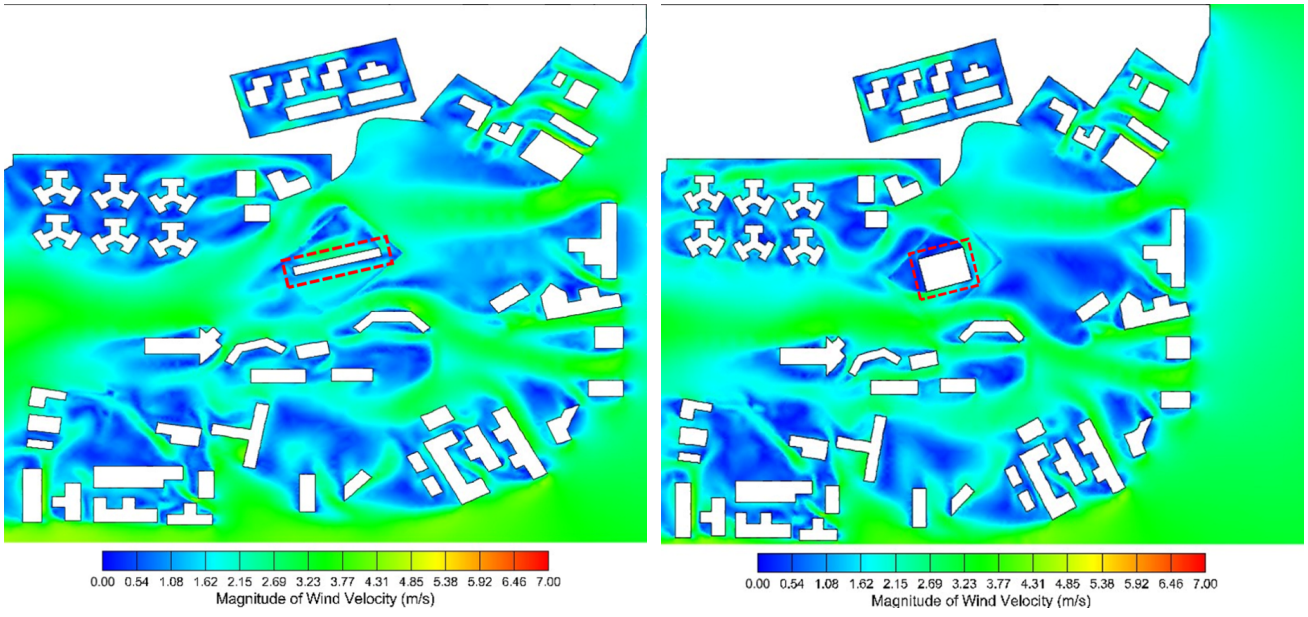

(a) Scenario 23 (b) Scenario 33

Fig. 10 Wind velocity distributions at z = 1.5 m of magnified view

significant mitigation of pedestrian thermal discomfort (D_{discom} decrease of 3.90 °C). The D_{discom} decrease of 2.10 °C is dominated by the increase of building orientation from 0° (Scenario 125) to 135° (Scenario 156). The increase of the aspect ratio from 1.4:1 (Scenario 33) to 9:1 (Scenario 23) dominates the D_{discom} decrease of 0.40 °C. The increase of the wall emissivity from 0.35 (Scenario 172) to 0.78 (Scenario 36) can mitigate the pedestrian thermal discomfort to 1.70 °C. When the overall heat transfer coefficient increases from 1.32 W/(m²·K) (Scenario 102) to 5.13 W/(m²·K) (Scenario 149), D_{discom} increases by 1.45 °C. The increase of heat rejection of air-conditioners from 96.64 W/m² (Scenario 123) to 145.23 W/m² (Scenario 2) can dominate the D_{discom} increase of 1.05 °C.

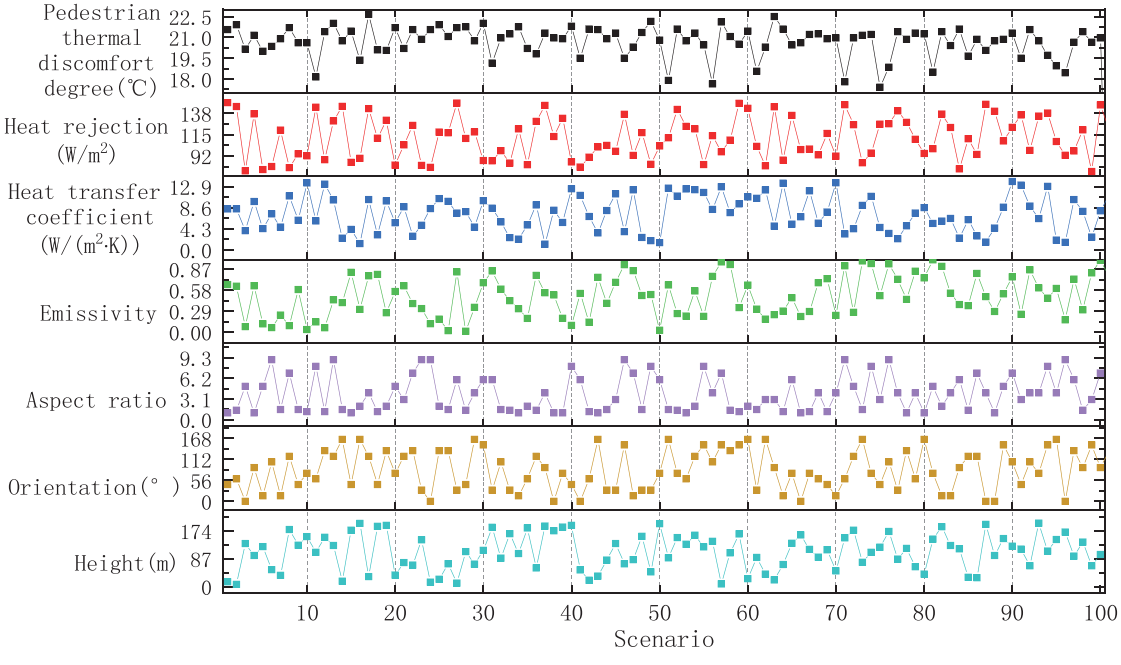

(a) Scenario 1 to Scenario 100

Fig. 11 Pedestrian thermal discomfort degrees under different scenarios

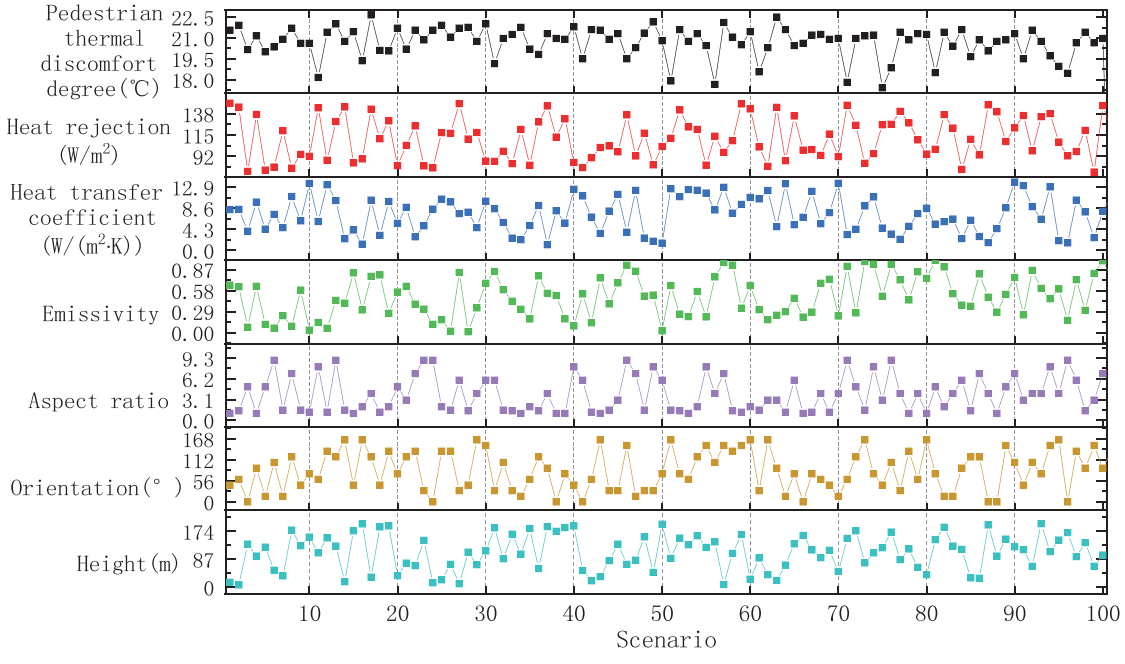

(b) Scenario 101 to Scenario 200

Fig. 11 Pedestrian thermal discomfort degrees under different scenarios (Continued)

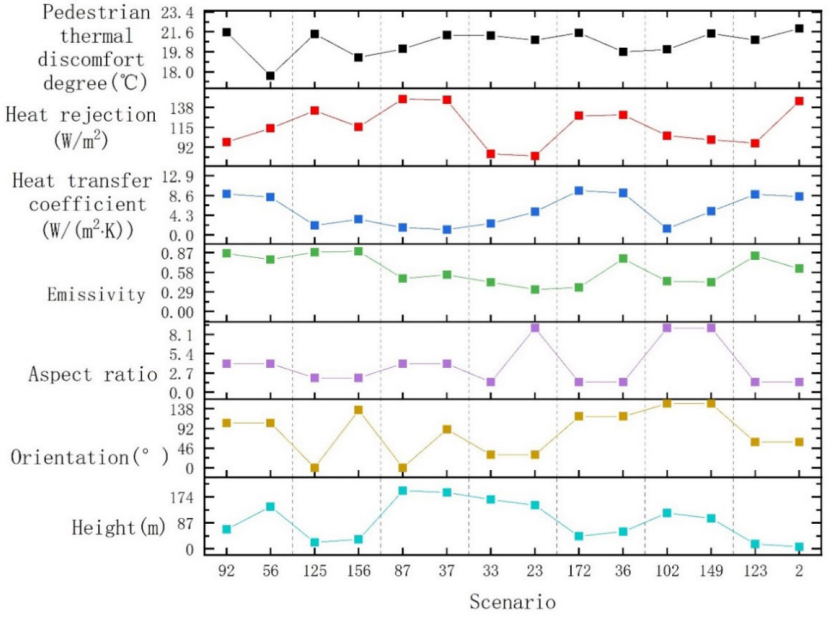

Fig. 12 Pedestrian thermal discomfort degrees of the district with the new building under different scenarios

4.2 Impacts of local microclimate on building energy performance

The differences between building energy consumptions considering local microclimate impacts and without considering the local microclimate impacts (i.e., under TMY weather) under the 200 scenarios of building design are shown in Figure 13, as well as the corresponding air temperature and wind velocity differences between the local microclimate and TMY weather. It can be seen that the air temperature difference between the local microclimate and TMY weather varies from +0.18 to +1.96 K under different building design scenarios, while the wind velocity difference varies within a range between −3.06 and +2.40 m/s. Among the 200 scenarios, all of the scenarios have a higher local air temperature than that of TMY weather, and 99.5% of the

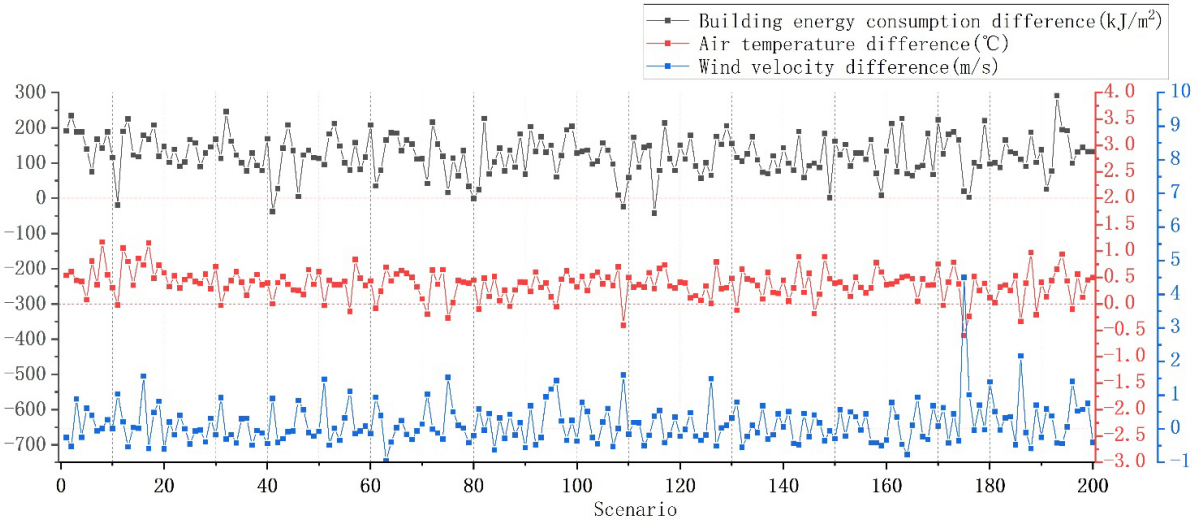

Fig. 13 Building energy consumption, outdoor air temperature and wind velocity differences between local microclimate and TMY under different scenarios

scenarios have a lower local wind velocity than that of TMY weather. The local microclimate can lead to an increase or decrease of building energy consumption within the range between −41.75 and +291.54 kJ/m^2 compared with the TMY weather. Only 2.5% of the scenarios has a decrease in the building energy consumption due to the microclimate impact. 91% of the scenarios has an increase in the building energy consumption larger than 50kJ/m^2. The average building energy consumption difference caused by local microclimate is 123.31 kJ/m^2. The highest building energy consumption increase happens when the air temperature difference is 1.49 K and the wind velocity difference is −2.74 m/s. When the air temperature difference is 1.12 K and the wind velocity difference is −2.05 m/s, there shows the largest decrease in the building energy consumption.

5 Identification of the major influential building parameters on both local microclimate and building energy consumption

5.1 Sensitivity analysis results

In this study, regression method, as a widely-used global sensitivity analysis method, is adopted. Spearman correlation coefficient (SPEA) is used to measure and compare the sensitivity of each building parameter to the four performance indexes introduced in Section 2.3 to identify the major influential parameters. A positive value means a positive correlation exists between the building parameters and the performance concerned, while a negative value means negative correlation. The larger the absolute value of SPEA is, the more sensitive the building parameter is to the performance.

Figure 14 shows the SPEA correlation coefficient between the six building parameters and the four performance indexes concerned. It can be seen that the building orientation and wall emissivity are the highly-sensitive parameters. The building orientation and overall heat transfer coefficient are positively correlated with the local air temperature difference, while the building height, aspect ratio, wall emissivity and heat rejection of air-conditioners are negatively correlated. This means that the increase in the building height, aspect ratio and wall emissivity would increase the ambient air temperature around the target building, while the increase in the overall heat transfer coefficient would decrease the ambient air temperature. These results are similar to those in previous studies concerning the impacts of district (Ignatius et al. 2015; Ali-Toudert and Böttcher 2018). The results are rational because the increase in the building height or aspect ratio would increase the shading around the building and the ambient wind velocity around the target building, and therefore decrease the ambient air temperature, which will mitigate thermal discomfort and reduce building energy consumption. The increase in the emissivity and the decrease in the heat transfer coefficient would lead to the less heat exchange and therefore a decrease in the ambient local air temperature, reducing both thermal discomfort and building energy consumption. The results regarding the heat rejection of air-conditioners seem inconsistent with previous studies where an increase of air temperature is observed around the condensing units of air-conditioners (Avara and Daneshgar 2008; Liu et al. 2019). This problem will be further discussed in Section 5.2. As for the local wind velocity difference, building height and aspect ratio are the highly-sensitive parameters. In general, the six

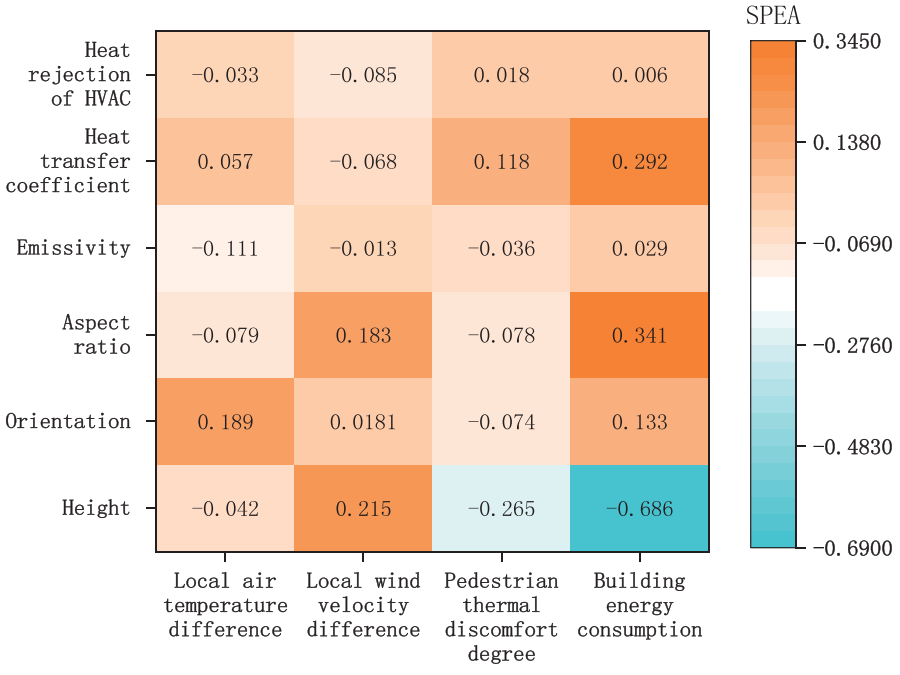

Fig. 14 SPEA correlation coefficient between building parameters and the performance indexes concerned

building parameters have more significant impacts on the local wind velocity than local air temperature. The building parameters that have positive impacts are the morphology parameters (i.e., building height, orientation, and aspect ratio), and the parameters that have negative impacts are the thermal characteristic parameters (i.e., wall emissivity, overall heat transfer coefficient, and air-conditioner heat rejection). Most of these results are similar to the previous studies. However, the result related to the building height is not consistent with that in previous studies concerning the impacts of district buildings (Ignatius et al. 2015; Ding and Lam 2019). The results are both rational due to the difference of the research scenarios concerned. In this study, the individual building is concerned. The increase in the building height would result in the higher ambient wind velocity and accelerate the ventilation around it. For the district buildings, the increase in the average building height would block the airflow of the district and thus decrease the wind velocity.

As for the pedestrian thermal discomfort degree, the building parameters that have positive impacts are overall heat transfer coefficient, and air-conditioner heat rejection. The parameters that have negative impacts are the morphology parameters and wall emissivity. Building height and overall heat transfer coefficient are the highly-sensitive parameters. Building height is the only parameter that has negative correlation with the building energy consumption considering local microclimate impacts. Building height, aspect ratio and overall heat transfer coefficient are the highly-sensitive parameters. However, in previous studies (Ali-Toudert and Böttcher 2018) regarding the impacts of district design, emissivity is recognized as the highly sensitive parameter, while the district aspect ratio has low impact. It is worth noting that the correlations between building parameters and local microclimate are relatively low compared with those with building energy consumption. This is because the building parameters which affect both the building performance and local microclimate are only considered, and the impacts of an individual building are limited compared with a whole district. However, the impacts of the relatively sensitive parameters (e.g., building height) cannot be ignored.

5.2 Discussion on the impacts of heat rejection of air-conditioners on local microclimate

It is worth noticing that the heat rejection of air-conditioners has negative correlations with the local air temperature and wind velocity differences, which seems inconsistent with theoretical inference. To further verify the rationality, a local sensitivity analysis of the air-conditioner heat rejection to the local microclimate is conducted by set other building parameters as fixed values. The local microclimate near the wall installed with air-conditioners, which is also the windward side, is particularly investigated, in view of stronger impacts near the air-conditioners. The windward-side local air temperature and wind velocity differences at 10 different distances (i.e., 0.1, 0.2, 0.3, 0.4, 0.5, 1.0, 1.5, 2.0, 2.5, 3.0 m)

from the new building in the horizontal direction is simulated under 20 different settings of heat rejection. The settings are determined according to the random sample from the corresponding range (i.e., 75–150 W/m^2). The results are shown in Figure 15.

It can be seen from Figure 15(a) that the air conditioner heat rejection increases the windward-side local air temperature at any distance concerned. The increase of the air conditioner heat rejection also leads to the increase of ambient air temperature difference when the distance is less than 0.5 m. When the microclimate at a further distance is concerned, the impacts of air-conditioner heat rejection become weak. Therefore, it is rational that the SPEA correlation coefficient between the heat rejection and local air temperature difference shown in Figure 14 is slightly negative, as it is calculated based on the average local air temperature differences of all sides at the distance of 3.0 m where the impacts become weak at a far distance and

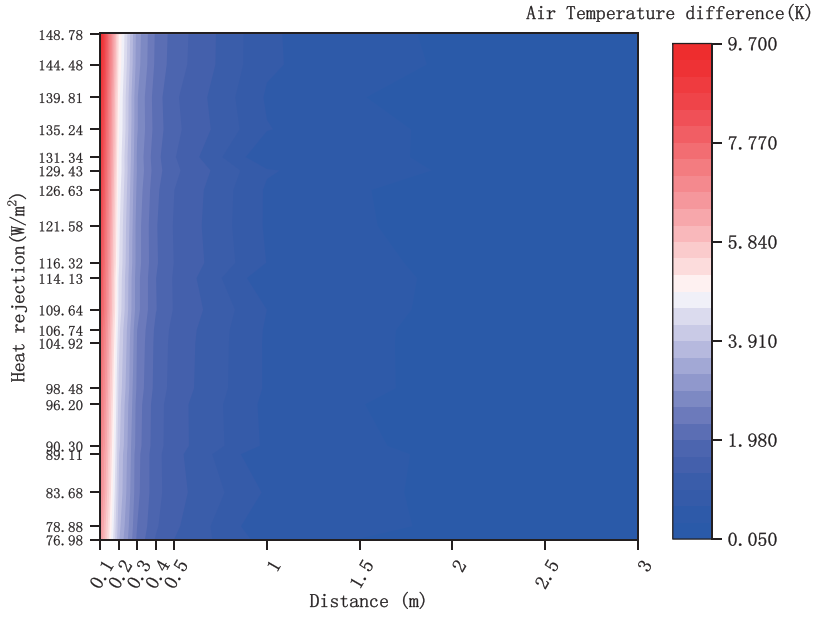

(a) Air temperature difference (K)

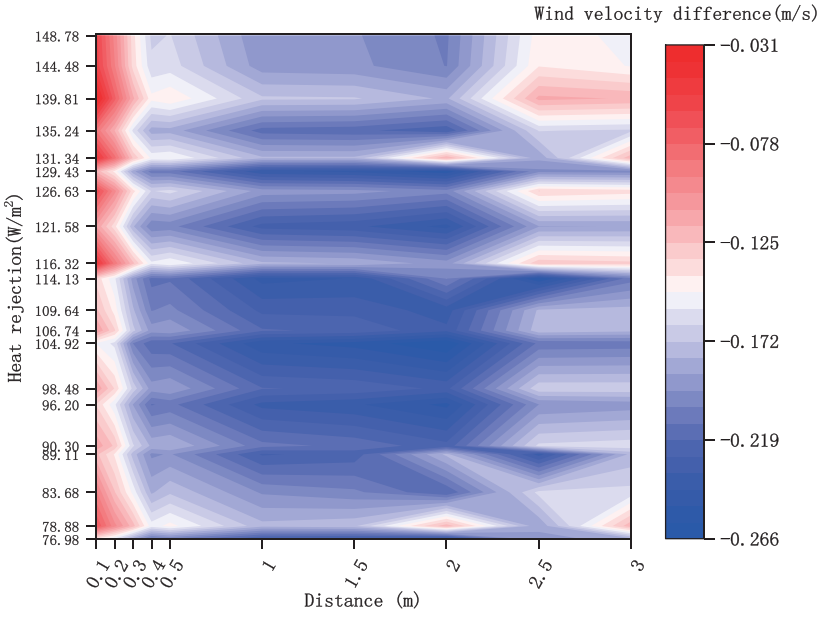

(b) Wind velocity difference (m/s)

Fig. 15 Windward-side local microclimate differences at different distances under different settings of air-conditioner heat rejection

complicated under the variation of all building parameters including building orientation. The windward-side local wind velocities at different distances are reduced due to the development of the new building as seen from Figure 15(b). But the local wind velocity difference does not show an obvious increase or decrease particularly at far distances when the air-conditioner heat rejection increases, due to insignificant impact of heat buoyancy force. Therefore, the slightly negative value of the SPEA correlation coefficient between the heat rejection and local wind velocity difference (shown in Figure 14) does not mean an obvious negative correlation, which is also applied for local air temperature difference.

5.3 Identification of the major influential building parameters

Based on the above sensitivity analysis results, the building parameters affecting the local air temperature and wind velocity are ranked respectively, as listed in Table 6(a). It can be seen that the ranking orders of the building parameters affecting local air temperature and wind velocity are totally different. The major influential building parameters on local air temperature are building orientation and wall emissivity, while the parameter with the least impact is the heat rejection of air-conditioners. The major influential building parameters on local wind velocity are building height and building aspect ratio, followed by the heat rejection of air-conditioners. The wall emissivity has the least impact on local wind velocity. It is worth noticing that the emissivity of wall and the heat rejection of air-conditioners, which are found to have significant impacts on local air temperature or wind velocity, are ignored in previous research.

As the pedestrian thermal comfort is widely used to evaluate the local microclimate, the building parameters affecting the pedestrian thermal discomfort degree are also ranked and compared with those affecting building energy consumption considering the microclimate impacts. The results are listed in Table 6(b). It can be seen that the major influential building parameters on pedestrian thermal discomfort degree are building height and overall heat transfer coefficient of building envelope, while the parameter with the least impact is the heat rejection of air conditioners. The ranking orders of the building parameters affecting building energy consumption are almost the same as those affecting pedestrian thermal discomfort degree, except for building orientation and overall heat transfer coefficient. The major influential parameters on building energy performance include building height, building aspect ratio, overall heat transfer coefficient of building envelope. It is recommended that the restrictions on the overall heat transfer coefficient of building envelope and building height specified in the building design guidelines or related policies should be given considering the impacts on both building energy consumption and local microclimate.

Although the ranking orders of the building parameters affecting pedestrian thermal discomfort and building energy consumption are similar, the correlations between the parameters and the performance are not the same. For instance, the building aspect ratio, building orientation and wall emissivity have negative correlations with pedestrian thermal discomfort, but positive correlations with the building energy consumption. Therefore, a building design which has the lowest building energy consumption is probably not friendly to the local microclimate. So it is necessary to consider the mutual impacts between building design and local microclimate in the design of new buildings to improve building energy performance while minimizing the impacts on the local microclimate.

Table 6(a) Ranking of major building parameters affecting local microclimate

	Performance	
Rank	Local air temperature	Local wind velocity
1	Building orientation	Building height
2	Emissivity of wall	Building aspect ratio
3	Building aspect ratio	Heat rejection of air-conditioners
4	Overall heat transfer coefficient of building envelope	Overall heat transfer coefficient of building envelope
5	Building height	Building orientation
6	Heat rejection of air-conditioners	Emissivity of wall

Table 6(b) Ranking of major building parameters affecting pedestrian thermal discomfort degree and building energy consumption considering microclimate impacts

	Performance	
Rank	Pedestrian thermal discomfort (correlation)	Building energy consumption (correlation)
1	Building height (negative)	Building height (negative)
2	Overall heat transfer coefficient of building envelope (positive)	Building aspect ratio (positive)
3	Building aspect ratio (negative)	Overall heat transfer coefficient of building envelope (positive)
4	Building orientation (negative)	Building orientation (positive)
5	Emissivity of wall (Negative)	Emissivity of wall (positive)
6	Heat rejection of air-conditioners (Positive)	Heat rejection of air-conditioners (positive)

6 Conclusions

In this study, a comprehensive and systematic analysis is conducted to investigate the mutual impacts between new individual building design and local microclimate considering their interaction in subtropical urban area, and to identify the major influential parameters on both local microclimate and building energy performance by sensitivity analysis. The mutual impact analysis and sensitivity analysis are based on 200 sets of microclimate and building performance simulations using advanced GIS-based spatial analysis techniques. Based on the analysis results, the major conclusions can be drawn and summarized as follows.

- Strong mutual impacts exist between the new building design and urban local microclimate. In this study, different building designs lead to significant variations of local wind velocity (i.e., −0.95 to +4.51 m/s), air temperature (i.e., −0.60 to +1.17 K), and pedestrian thermal discomfort degree (i.e., 13.75 to 22.65 °C). The local microclimate results in a change in the building energy consumption from −41.75 to 291.54 kJ/m^2.
- The major influential parameters on local air temperature, wind velocity and pedestrian thermal discomfort are rather different. The major influential parameters on local air temperature are building orientation and wall emissivity, while the major influential parameters on local wind velocity are building height and aspect ratio. As for the pedestrian thermal discomfort, the major influential parameters include building height and overall heat transfer coefficient of building envelope.
- The major influential parameters on both local microclimate and building energy performance are building height and overall heat transfer coefficient of building envelope. Although the ranking orders of the building parameters affecting pedestrian thermal discomfort and building energy consumption are similar, the correlations between the parameters and the performance are significantly different. Therefore, it is necessary to consider the mutual impacts between building design and local microclimate in the design of new buildings to improve building energy performance while minimizing the impacts on the local microclimate.

The general findings in this study can all be applied to other types of buildings in high-density cities, except for the findings concerning the impacts of heat rejection of air-conditioners. This is because window type air-conditioners are usually adopted in dormitory buildings, and their impacts on ambient environment could be very different from those of buildings adopting central cooling systems. The outcomes of this study can provide the basis for the consideration of mutual impacts between buildings and local microclimate in new building or rebuilding design at the early stage to facilitate carbon neutrality and enhance thermal comfort in urban area.

7 Limitations

In this study, the thermal characteristics of the building for building performance simulation in EnergyPlus, such as the specific heat capacity, density, thickness, thermal absorptance, solar absorptance, and visible absorptance, are assumed as constant values, the impacts of which on the microclimate are ignored and could be investigated in future work. The representation of trees and roads in the study area is simplified to save computational resources.

Acknowledgements

The research work presented in this paper is funded by Shenzhen Science and Technology Innovation Commission (Grant No. KCXST20221021111203007) and General Research Grant (15221623) of the Research Grant Council (RGC) of the Hong Kong SAR, China.

Funding note: Open access funding provided by The Hong Kong Polytechnic University.

Declaration of competing interest

The authors have no competing interests to declare that are relevant to the content of this article. Shengwei Wang is an Editorial Board member of *Building Simulation.*

Author contribution statement

Conceptualization, methodology, software, validation, formal analysis and writing—original draft were performed by Zeming Zhao. Conceptualization, methodology, writing—review & editing, supervision, project administration and funding acquisition were performed by Hangxin Li. Writing—review & editing, supervision, project administration and funding acquisition were performed by Shengwei Wang.

References

Ali-Toudert F, Mayer H (2006). Numerical study on the effects of aspect ratio and orientation of an urban street canyon on outdoor thermal comfort in hot and dry climate. *Building and Environment*, 41: 94–108.

Ali-Toudert F, Böttcher S (2018). Urban microclimate prediction prior to dynamic building energy modelling using the TEB model as embedded component in TRNSYS. *Theoretical and Applied Climatology*, 134: 1413–1428.

Allegrini J, Dorer V, Carmeliet J (2012). Influence of the urban microclimate in street canyons on the energy demand for space cooling and heating of buildings. *Energy and Buildings*, 55: 823–832.

Allegrini J, Dorer V, Carmeliet J (2015). Influence of morphologies on the microclimate in urban neighbourhoods. *Journal of Wind Engineering and Industrial Aerodynamics*, 144: 108–117.

Allegrini J, Carmeliet J (2017). Coupled CFD and building energy simulations for studying the impacts of building height topology and buoyancy on local urban microclimates. *Urban Climate*, 21: 278–305.

Allegrini J, Carmeliet J (2018). Simulations of local heat islands in Zürich with coupled CFD and building energy models. *Urban Climate*, 24: 340–359.

Allen-Dumas MR, Sweet LT, Brelsford C (2022). Determining optimal resolution for urban terrain inputs to microclimate modeling. ESS Open Archive. https://doi.org/10.1002/essoar.10507082.1

Avara A, Daneshgar E (2008). Optimum placement of condensing units of split-type air-conditioners by numerical simulation. *Energy and Buildings*, 40: 1268–1272.

Back Y, Kumar P, Bach PM, et al. (2023). Integrating CFD-GIS modelling to refine urban heat and thermal comfort assessment. *Science of the Total Environment*, 858: 159729.

Bourbia F, Boucheriba F (2010). Impact of street design on urban microclimate for semi arid climate (Constantine). *Renewable Energy*, 35: 343–347.

Bueno B, Norford L, Hidalgo J, et al. (2013). The urban weather generator. *Journal of Building Performance Simulation*, 6: 269–281.

Bueno B, Roth M, Norford L, et al. (2014). Computationally efficient prediction of canopy level urban air temperature at the neighbourhood scale. *Urban Climate*, 9: 35–53.

Buildings Department (2014). Guidelines on design and construction requirements for energy efficiency of residential buildings. Available at https://www.bd.gov.hk/doc/en/resources/codes-and-references/code-and-design-manuals/Guidelines_DCREERB2014e.pdf.

Chen L, Hang J, Sandberg M, et al. (2017). The impacts of building height variations and building packing densities on flow adjustment and city breathability in idealized urban models. *Building and Environment*, 118: 344–361.

Chow TT, Lin Z, Yang XY (2002). Placement of condensing units of split-type air-conditioners at low-rise residences. *Applied Thermal Engineering*, 22: 1431–1444.

Cui Y, Yan D, Hong T, et al. (2017). Temporal and spatial characteristics of the urban heat island in Beijing and the impact on building design and energy performance. *Energy*, 130: 286–297.

Deng X, Nie W, Li X, et al. (2023). Influence of built environment on outdoor thermal comfort: A comparative study of new and old urban blocks in Guangzhou. *Building and Environment*, 234: 110133.

Dimoudi A, Kantzioura A, Zoras S, et al. (2013). Investigation of urban microclimate parameters in an urban center. *Energy and Buildings*, 64: 1–9.

Ding C, Lam KP (2019). Data-driven model for cross ventilation potential in high-density cities based on coupled CFD simulation and machine learning. *Building and Environment*, 165: 106394.

Diz-Mellado E, Ruiz-Pardo Á, Rivera-Gómez C, et al. (2023). Unravelling the impact of courtyard geometry on cooling energy consumption in buildings. *Building and Environment*, 237: 110349.

Franke J, Hellsten A, Schlünzen H, et al. (2007). Best practice guideline for the CFD simulation of flows in the urban environment. *COST Action*, 44: 1–52.

Ge J, Wang Y, Zhou D, et al. (2023). Building energy demand of urban blocks in Xi'an, China: impacts of high-rises and vertical meteorological pattern. *Building and Environment*, 244: 110749.

Guattari C, Evangelisti L, Balaras CA (2018). On the assessment of urban heat island phenomenon and its effects on building energy performance: A case study of Rome (Italy). *Energy and Buildings*, 158: 605–615.

Hang J, Li Y (2010). Ventilation strategy and air change rates in idealized high-rise compact urban areas. *Building and Environment*, 45: 2754–2767.

Ignatius M, Wong NH, Jusuf SK (2015). Urban microclimate analysis with consideration of local ambient temperature, external heat gain, urban ventilation, and outdoor thermal comfort in the tropics. *Sustainable Cities and Society*, 19: 121–135.

Inanici MN, Demirbilek FN (2000). Thermal performance optimization of building aspect ratio and south window size in five cities having different climatic characteristics of Turkey. *Building and Environment*, 35: 41–52.

Kong M, Yu M, Liu N, et al. (2017). Combined GIS, CFD and neural network multi-zone model for urban planning and building simulation. In: Proceedings of the 15th International IBPSA Building Simulation Conference, San Francisco, CA, USA.

Lee G, Jeong Y (2017). Impact of urban and building form and microclimate on the energy consumption of buildings based on statistical analysis. *Journal of Asian Architecture and Building Engineering*, 16: 565–572.

Li H, Wang S, Cheung H (2018). Sensitivity analysis of design parameters and optimal design for zero/low energy buildings in subtropical regions. *Applied Energy*, 228: 1280–1291.

Li Y, Ouyang W, Yin S, et al. (2023). Microclimate and its influencing factors in residential public spaces during heat waves: An empirical study in Hong Kong. *Building and Environment*, 236: 110225.

Lin M, Hang J, Li Y, et al. (2014). Quantitative ventilation assessments of idealized urban canopy layers with various urban layouts and the same building packing density. *Building and Environment*, 79: 152–167.

Liu J, Heidarinejad M, Nikkho SK, et al. (2019). Quantifying impacts of urban microclimate on a building energy consumption—a case study. *Sustainability*, 11: 4921.

Mao J, Yang JH, Afshari A, et al. (2017). Global sensitivity analysis of an urban microclimate system under uncertainty: design and case study. *Building and Environment*, 124: 153–170.

Mao J, Fu Y, Afshari A, et al. (2018). Optimization-aided calibration of an urban microclimate model under uncertainty. *Building and Environment*, 143: 390–403.

Martilli A, Santiago JL, Martín F (2007). Micrometeorological modelling in urban areas. *Física de la Tierra*, 133(19): 133–145.

Merlier L, Frayssinet L, Johannes K, et al. (2019a). On the impact of local microclimate on building performance simulation. Part I: prediction of building external conditions. *Building Simulation*, 12: 735–746.

Merlier L, Frayssinet L, Johannes K, et al. (2019b). On the impact of local microclimate on building performance simulation. Part II: effect of external conditions on the dynamic thermal behavior of buildings. *Building Simulation*, 12: 747–757.

Middel A, Häb K, Brazel AJ, et al. (2014). Impact of urban form and design on mid-afternoon microclimate in Phoenix Local Climate Zones. *Landscape and Urban Planning*, 122: 16–28.

Mohammad AF, Ahmad Zaki S, Ali MSM, et al. (2015). Large eddy simulation of wind pressure distribution on heterogeneous buildings in idealised urban models. *Energy Procedia*, 78: 3055–3060.

Mosteiro-Romero M, Maiullari D, Pijpers-van Esch M, et al. (2020). An integrated microclimate-energy demand simulation method for the assessment of urban districts. *Frontiers in Built Environment*, 6: 553946.

Mutani G, Fiermonte F (2016). Microclimate models for a sustainable and liveable urban planning. In: Ingaramo R, Voghera A (eds), Topics and Methods for Urban and Landscape Design: From the River to the Project. Cham, Switzerland: Springer International Publishing.

Ng E, Cheng V (2012). Urban human thermal comfort in hot and humid Hong Kong. *Energy and Buildings*, 55: 51–65.

Palme M, Inostroza L, Villacreses G, et al. (2017). From urban climate to energy consumption. Enhancing building performance simulation by including the urban heat island effect. *Energy and Buildings*, 145: 107–120.

Paolini R, Zani A, MeshkinKiya M, et al. (2017). The hygrothermal performance of residential buildings at urban and rural sites: sensible and latent energy loads and indoor environmental conditions. *Energy and Buildings*, 152: 792–803.

Potchter O, Cohen P, Lin TP, et al. (2018). Outdoor human thermal perception in various climates: A comprehensive review of approaches, methods and quantification. *Science of the Total Environment*, 631: 390–406.

Salvati A, Coch Roura H, Cecere C (2017). Assessing the urban heat island and its energy impact on residential buildings in Mediterranean climate: Barcelona case study. *Energy and Buildings*, 146: 38–54.

Sezer N, Yoonus H, Zhan D, et al. (2023). Urban microclimate and building energy models: A review of the latest progress in coupling strategies. *Renewable and Sustainable Energy Reviews*, 184: 113577.

Shen P, Liu J, Wang M (2021). Fast generation of microclimate weather data for building simulation under heat island using map capturing and clustering technique. *Sustainable Cities and Society*, 71: 102954.

Shi L, Luo Z, Matthews W, et al. (2019). Impacts of urban microclimate on summertime sensible and latent energy demand for cooling in residential buildings of Hong Kong. *Energy*, 189: 116208.

Sun L, Chen J, Li Q, et al. (2020). Dramatic uneven urbanization of large cities throughout the world in recent decades. *Nature Communications*, 11: 5366.[PubMed]

GB/T 51350 (2019). GB/T 51350-2019: Technical Standard for Near Zero Energy Buildings. (in Chinese)

Theeuwes NE, Steeneveld GJ, Ronda RJ, et al. (2014). Seasonal dependence of the urban heat island on the street canyon aspect ratio. *Quarterly Journal of the Royal Meteorological Society*, 140: 2197–2210.

Tominaga Y, Mochida A, Shirasawa T, et al. (2004). Cross comparisons of CFD results of wind environment at pedestrian level around a high-rise building and within a building complex. *Journal of Asian Architecture and Building Engineering*, 3: 63–70.

Tominaga Y, Yoshie R, Mochida A, et al. (2005). Cross comparisons of CFD prediction for wind environment at pedestrian level around buildings. Part 2: Comparison of results for flow field around building complex in actual urban area. In: Proceedings of the 6th Asian-Pacific Conference on Wind Engineering (APCWE-Vi), Seoul, R.O. Korea.

Tominaga Y, Mochida A, Yoshie R, et al. (2008). AIJ guidelines for practical applications of CFD to pedestrian wind environment around buildings. *Journal of Wind Engineering and Industrial Aerodynamics*, 96: 1749–1761.

Tsoka S (2017). Investigating the relationship between urban spaces morphology and local microclimate: A study for Thessaloniki. *Procedia Environmental Sciences*, 38: 674–681.

Wang L, Wu L, Norford LK, et al. (2024). The interactive indoor-outdoor building energy modeling for enhancing the predictions of urban microclimates and building energy demands. *Building and Environment*, 248: 111059.

Wang R, Ren C, Xu Y, et al. (2018). Mapping the local climate zones of urban areas by GIS-based and WUDAPT methods: a case study of Hong Kong. *Urban Climate*, 24: 567–576.

Yassin MF (2013). Numerical modeling on air quality in an urban environment with changes of the aspect ratio and wind direction. *Environmental Science and Pollution Research International*, 20: 3975–3988.[PubMed]

Xie X, Sahin O, Luo Z, et al. (2020). Impact of neighbourhood-scale climate characteristics on building heating demand and night ventilation cooling potential. *Renewable Energy*, 150: 943–956.

Zhao Z, Li H, Wang S (2022). Identification of the key design parameters of Zero/low energy buildings and the impacts of climate and building morphology. *Applied Energy*, 328: 120185.

Zinzi M, Carnielo E, Mattoni B (2018). On the relation between urban climate and energy performance of buildings. A three-years experience in Rome, Italy. *Applied Energy*, 221: 148–160.